PREPRINT

Three-dimensional anatomy of the early Eocene †*Whitephippus* (Teleostei: Lampriformes) documents parallel conquests of the pelagic environment by multiple teleost lineages

Donald Davesne[1,2*], James V. Andrews[3,4,*], Hermione T. Beckett[2,5], Sam Giles[6], Matt Friedman[3,4]

[1]Museum für Naturkunde, Leibniz-Institut für Evolutions- und Biodiversitätsforschung, 10115 Berlin, Germany
[2]Deparment of Earth Sciences, University of Oxford, Oxford OX1 3AN, UK
[3]Department of Earth & Environmental Sciences, University of Michigan, Ann Arbor, Michigan 48109- 1382, USA
[4]Museum of Paleontology, University of Michigan, Ann Arbor, Michigan 48109- 1382, USA
[5]Department of Biology, King's High School for Girls, Warwick, UK
[6]School of Geography Earth and Environmental Sciences, University of Birmingham, Birmingham B15 2TT, UK
[*]DD and JVA contributed equally to this work.
Corresponding authors: Donald Davesne (donald.davesne@gmail.com), James V. Andrews (jamesva@umich.edu)
ORCID numbers: Donald Davesne https://orcid.org/0000-0002-4775-2360, James V. Andrews https://orcid.org/0000-0001-7093-1335, Hermione T. Beckett https://orcid.org/0000-0003-4475-021X, Sam Giles https://orcid.org/0000-0001-9267-4392, Matt Friedman https://orcid.org/0000-0002-0114-7384

ABSTRACT
The early Eocene fossil assemblage of the London Clay (Southeastern England) is a key window to the early Palaeogene diversification of teleost fishes in the open ocean. Despite their three-dimensional preservation that offers unique insight into skeletal anatomy, the London Clay fossils are still poorly described for the most part. †*Whitephippus tamensis* is a fossil teleost from this assemblage, known by several well-preserved specimens. Based on a complete description of the known material, including hidden structures (braincase, hyoid and branchial arches) revealed through 3D microtomography, we reinterpret †*Whitephippus* as an early member of the teleost group Lampriformes. More specifically, the anatomy of †*Whitephippus* indicates that it is likely a member of the so-called 'pelagic clade' including modern opahs and oarfishes. This redescription of †*Whitephippus* provides the earliest definitive evidence of lampriforms conquering the pelagic environment, alongside numerous other teleost lineages.

Key words: Eocene, London Clay, Teleostei, Acanthomorpha, Lampriformes, computed tomography

INTRODUCTION

Actinopterygians (ray-finned fishes) are the primary vertebrate component of open-ocean ecosystems. The Cretaceous-Palaeogene extinction event shaped this modern diversity by selectively affecting large predatory pelagic actinopterygian taxa, such as pachycormiforms, ichthyodectiforms, pachyrhizodontids and large aulopiforms (Cavin, 2001; Friedman, 2009; Friedman & Sallan, 2012). Their ecological equivalents in the modern ocean are mostly spiny-rayed teleosts (acanthomorphs) such as scombrids (e.g., tunas), xiphioids (billfishes) and carangoids (e.g., jacks and dolphinfishes). Although they all represent distinct evolutionary lineages, these groups of fast-swimming predators share gross similarities like streamlined bodies and falcate caudal fins.

Evidence from the fossil record (Friedman, 2010; Friedman & Sallan, 2012; Guinot & Cavin, 2016) and node-dated molecular studies (Alfaro et al., 2018, 2009; Ghezelayagh et al., 2022; Harrington et al., 2016; Miya et al., 2013) suggest that acanthomorph lineage diversity and body shape disparity exploded in the early Palaeogene. Pelagic taxa in particular have been proposed to represent a case of parallel adaptive radiations, triggered by the conquest of ecological niches left vacant by the Cretaceous-Palaeogene extinction event (Friedman, 2010; Miya et al., 2013). The most prominent groups of pelagic predatory acanthomorphs have their earliest appearances clustered in a relatively short time interval in the late Paleocene-early Eocene (Fierstine, 2006; Monsch & Bannikov, 2011; Santini & Carnevale, 2015; Santini, Carnevale, & Sorenson, 2013). A relatively low number of fossil sites document teleost diversity in the open ocean during this key time interval (Argyriou & Davesne, 2021; Friedman, Beckett, Close, & Johanson, 2016).

The London Clay of Southeastern England is one of these fossil localities. This Ypresian (early Eocene, c. 52-49 Ma) assemblage preserves a very diverse marine teleost fauna with very few equivalents in the early Palaeogene in terms of taxonomic richness (Casier, 1966; Friedman et al., 2016). Its composition closely matches that of modern open ocean faunas, with taxa like scombrids (Beckett & Friedman, 2016; Monsch, 2005), xiphioids (Monsch, 2005), luvarids (Bannikov & Tyler, 1995), megalopids (Forey, 1973), trichiuroids (Beckett, Giles, Johanson, & Friedman, 2018) and carangids (Casier, 1966; Friedman et al., 2016; Monsch, 2005). Remarkably, teleosts from the London Clay are preserved in three dimensions, with minimal deformation and fine internal and external anatomical details in life position. These unique taphonomic conditions offer the possibility to study phylogenetically informative anatomical structures that would usually be concealed in flattened fossils, such as the braincase and branchial arches (e.g. Beckett & Friedman 2016; Close *et al.* 2016; Friedman *et al.* 2016; Beckett *et al.* 2018). The diversity of the London Clay fauna has been noted as early as the 19th century (e.g., Agassiz 1845), described by Woodward (1901) and later revised in details by Casier (1966). However, some of the taxa referred to in these publications are probably misclassified (Patterson, 1993), and the phylogenetic positions of most are poorly constrained (Friedman et al., 2016).

†*Whitephippus* is one such case. This genus, known by several specimens (Figs. 1-4), has been attributed to the extant family Ephippidae (spadefishes) by Woodward (1901) and Casier (1966). However, some authors (Bonde, 1995; Carnevale, 2004; Friedman et al., 2016) have proposed that †*Whitephippus* should be classified with Lampriformes instead. Lampriformes are a clade of marine pelagic acanthomorphs that include such distinctive taxa as the endothermic opah (Lampridae) and the giant elongated oarfish (Regalecidae). Lampriform fossil taxa are relatively numerous, documenting the extreme morphological changes underwent in the early evolution of

the group (Bannikov, 1999, 2014; Davesne, 2017; Davesne et al., 2014). Significantly, †*Whitephippus* is the only fossil lampriform known by complete and three-dimensionally preserved skulls (Figs. 1-2). Using computed microtomography (µCT-scan), we reevaluate the anatomy and phylogenetic position of †*Whitephippus*, giving a unique perspective of the evolution of lampriforms in the context of the origin of modern pelagic actinopterygian faunas.

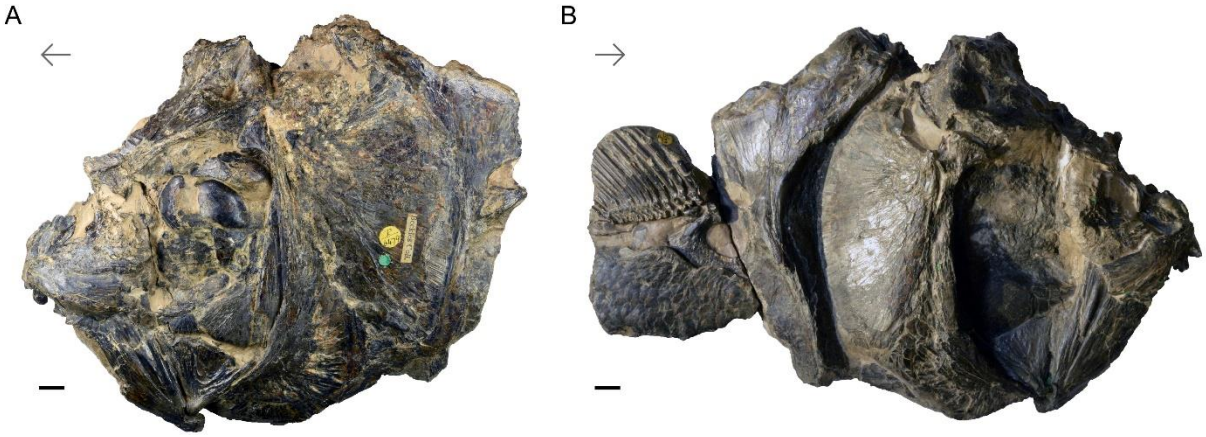

Figure 1. †*Whitephippus tamensis* holotype. NHMUK PV P 6479, London Clay Formation, early Eocene (Ypresian), Southeast England, UK. Photographs of specimen in (**A**) left and (**B**) right lateral views. Arrows indicate anatomical anterior. Scale bars represent 1 cm.

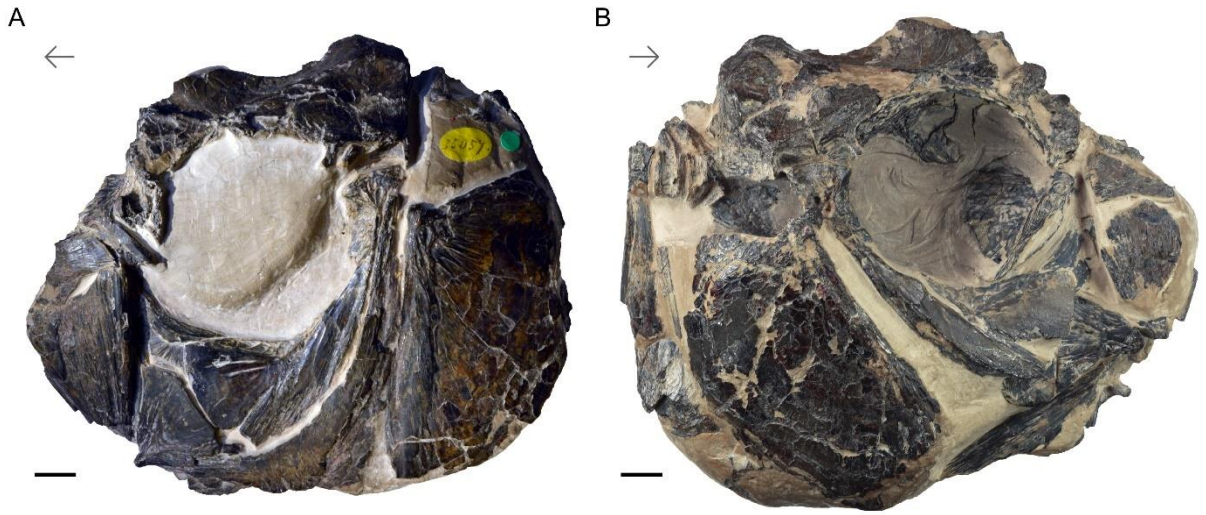

Figure 2. †*Whitephippus tamensis*. NHMUK PV P 35057, London Clay Formation, early Eocene (Ypresian), Southeast England, UK. Photographs of specimen in (**A**) left and (**B**) right lateral views. Arrows indicate anatomical anterior. Scale bars represent 1 cm.

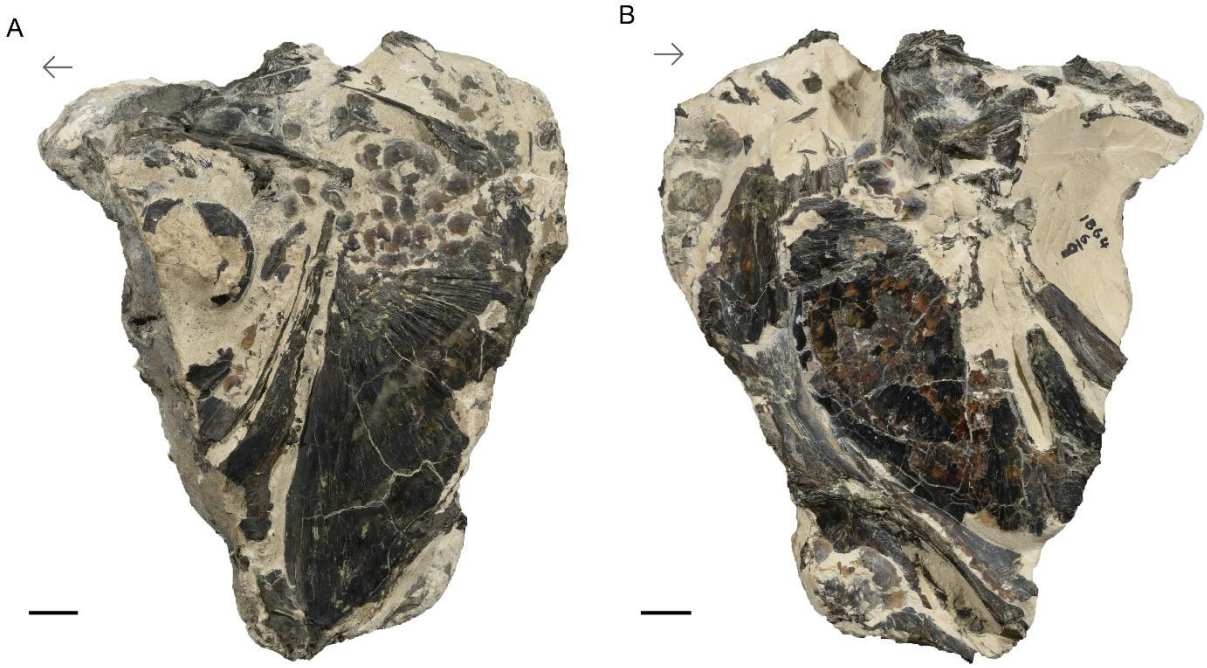

Figure 3. †*Whitephippus tamensis*. NMS 1864.6.9, London Clay Formation, early Eocene (Ypresian), Southeast England, UK. Photographs of specimen in (**A**) left and (**B**) right lateral views. Arrows indicate anatomical anterior. Scale bars represent 1 cm.

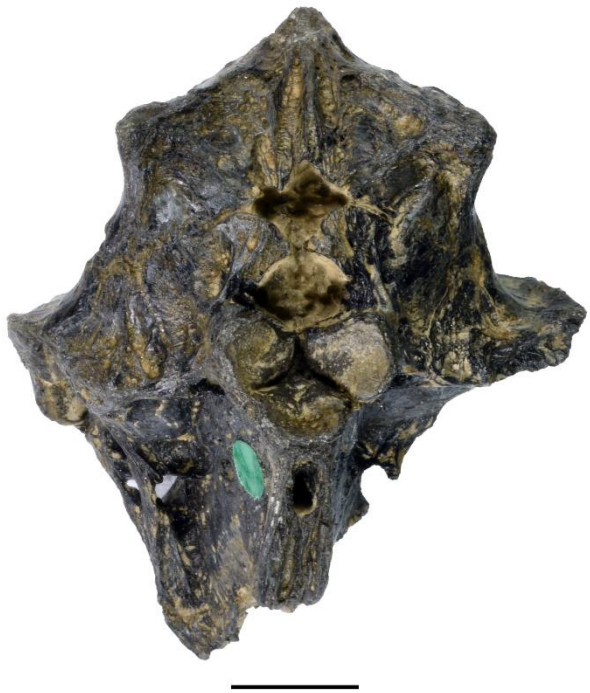

Figure 4. †*Whitephippus tamensis*. NHMUK PV 41384, London Clay Formation, early Eocene (Ypresian), Southeast England, UK. Neurocranium in posterior view. Scale bar represents 1 cm.

MATERIAL AND METHODS

Specimen imaging

Computed tomography. NHMUK fossil specimens were imaged using the Nikon XT H 225 ST industrial CT scanner at the Natural History Museum, London. Reconstructed datasets were segmented and visualized in Mimics v 19.0 (Materialise, Belgium). A fossil specimen from NMS and a recent specimen from UMMZ were imaged using the

same model of instrument in the CTEES facility at the University of Michigan. Osteological figures were generated in Blender v 2.91 (blender.org) from surface (.ply) files. The surface files of segmented elements are available on MorphoSource (URL to be provided after acceptance).

Institutional abbreviations
Institutional abbreviations follow those of Sabaj (2020). **AMNH**, American Museum of Natural History, New York, NY, USA; **MNHN**, Muséum national d'Histoire naturelle, Paris, France; **NHMUK**, Natural History Museum, London, UK; **NMS**, National Museums of Scotland, Edinburgh, UK; **ZMUC-P**, Statens Naturhistoriske Museum (SNM), Københavns Universitet, Copenhagen, Denmark.

Dagger symbol
The obelus (†) indicates extinct taxa, following Patterson & Rosen (1977).

Comparative material:
Fossil:
†*Whitephippus tamensis*, NHMUK PV P 6479, holotype, almost complete cranium with parts of the pectoral girdle and fin (µCT-scanned);
†*Whitephippus tamensis*, NHMUK PV 41384, paratype, isolated posterior portion of the neurocranium;
†*Whitephippus* cf. *tamensis*, NMS 1864.6.9, posterior portion of the cranium, vertebrae and pectoral girdle (µCT-scanned).
†*Whitephippus* cf. *tamensis*, NHMUK PV OR 35057, almost complete cranium (µCT-scanned);

Extant:
Lampris guttatus, AMNHN 79669 SD, 21720 SD, MNHN.ZA.1883-1795, ZMUC 74 (dry osteological preparations; specific attribution follows that accompanying these materials, and we acknowledge that these might belong to other species of *Lampris*; Underkoffler *et al.* 2018); *Metavelifer multiradiatus*, AMNH 214663 SD, 219280 SD, 91808 SD, 91800 SD and 91798 SD (dry osteological preparations); *Velifer hypselopterus*, MNHN.IC.1982.0025, UMMZ 220456 (preserved in alcohol and µCT-scanned).

SYSTEMATIC PALAEONTOLOGY

TELEOSTEI Müller, 1845
ACANTHOMORPHA Rosen, 1973
Order LAMPRIFORMES Goodrich, 1909
Genus †*WHITEPHIPPUS* Casier, 1966

†*Whitephippus tamensis* Casier, 1966

1901 †*Laparus alticeps* Woodward, p. 596
1966 †*Whitephippus tamensis* Casier, p. 237-243, figs. 52-54, pl. 31

Holotype. NHMUK PV P 6479.
Paratype. NHMUK PV 41384.

Type locality. Isle of Sheppey, Kent, England, United Kingdom.

Stratigraphic age. London Clay Formation, unit D (King, 1981, 1984). Ypresian, early Eocene, c. 52-49 Ma.

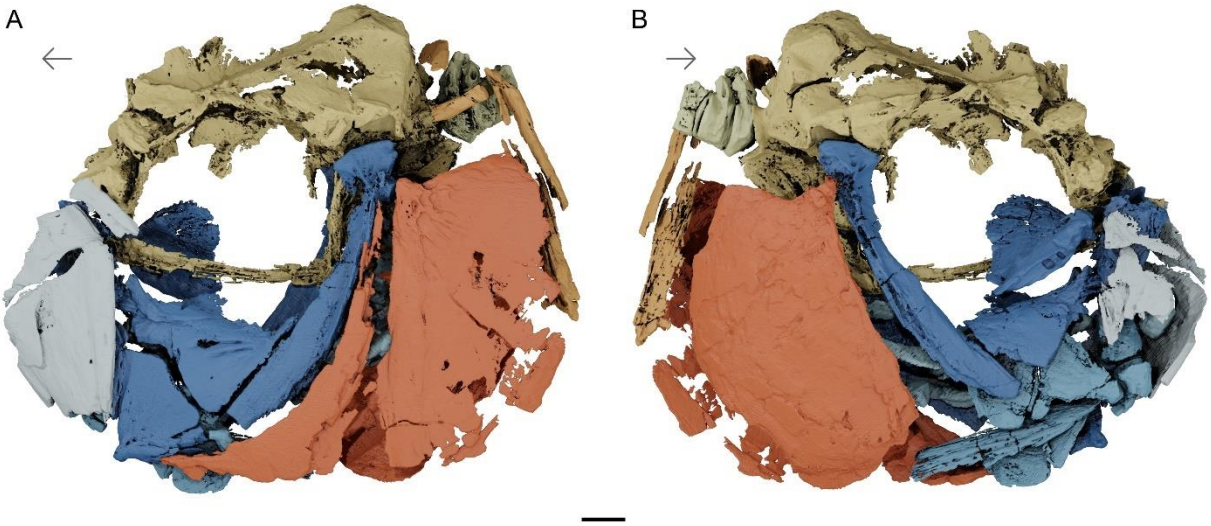

Figure 5. Skull of †*Whitephippus tamensis*. NHMUK PV P 35057, London Clay Formation, early Eocene (Ypresian), Southeast England, UK. Rendered µCT models showing the (**A**) left and (**B**) right sides of the skull. Skeletal regions highlighted as follows: neurocranium (yellow), suspensorium (dark blue), jaws (platinum), opercles (sienna), ventral hyoid (blue), gill skeleton (light blue), pectoral girdle (orange), vertebral column (light yellow). Arrows indicate anatomical anterior. Scale bar represents 1 cm.

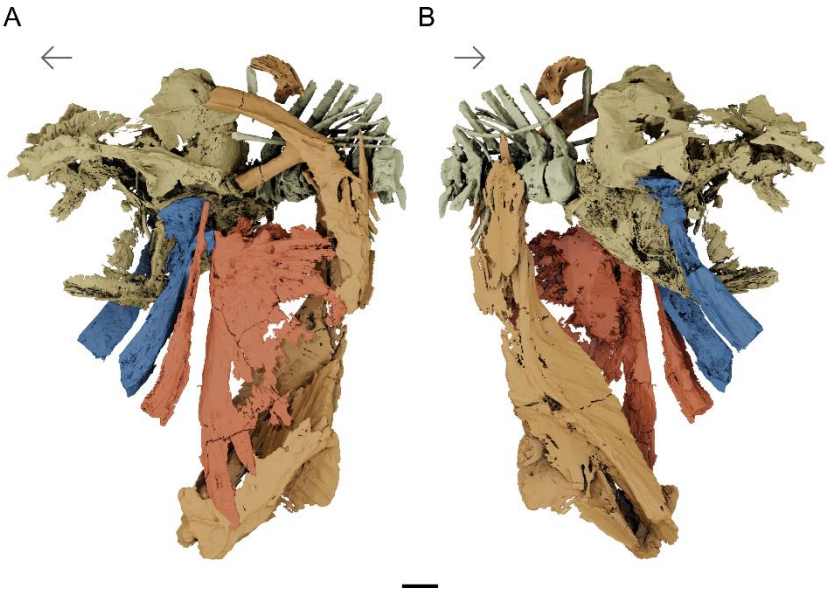

Figure 6. Skull, vertebrae, and pectoral girdle of †*Whitephippus tamensis*. NMS 1864.6.9, London Clay Formation, early Eocene (Ypresian), Southeast England, UK. Rendered µCT models showing the (**A**) left and (**B**) right sides of the specimen. Skeletal regions highlighted as follows: neurocranium (yellow), suspensorium (dark blue), jaws (platinum), opercles (sienna), ventral hyoid (blue), gill skeleton (light blue), pectoral girdle (orange), vertebral column (light yellow). Arrows indicate anatomical anterior. Scale bar represents 1 cm.

Description

Neurocranium

No specimen of †*Whitephippus* preserves a complete neurocranium. NHMUK PV 41384 represents an isolated neurocranium that is incomplete and largely free of surrounding matrix (Fig. 4). The neurocranium is incompletely exposed in NMS 1864.6.9, NHMUK PV P6479 and NHMUK PV 35057 (Figs. 1-3), but µCT reveals considerable detail of concealed anatomy in the latter. Our description of the neurocranium draws on all four specimens.

Anteriorly, the neurocranium includes a mesethmoid and paired lateral ethmoids that are tightly bound to one another (Figs. 5, 7). The junction between these bones is clear dorsally, where they are separated by a conspicuous vertical suture; they cannot be distinguished from one another more ventrally. The lateral ethmoid defines the anterior margin of the orbit, and its anterior and posterior surface are concave. The foramen for the olfactory nerve pierces the lateral ethmoid in its ventral half, near to the bone's junction with the mesethmoid. Viewed anteriorly, the outer margins of the lateral ethmoids are strongly excavated at the level of this canal. The anterolateral corner of the lateral ethmoid articulates with the lacrimal (infraorbital 1).

The dorsal surface of the mesethmoid forms a trough (Fig. 7). The mesethmoid extends slightly posterior to the lateral ethmoids when viewed laterally. The broad dorsal groove of the mesethmoid forms the floor of an open chamber, defined laterally by the broken edge of the frontals. Viewed dorsally, this chamber is 'V' shaped, with its apex pointing posteriorly. The incomplete frontals are folded dorsally over their anterior third, such that their exterior surfaces face laterally. We interpret this arrangement as representing a broken frontal 'vault' that would have opened anteriorly but been enclosed laterally and dorsally. This vault accommodates the greatly elongated ascending processes of the premaxillae in extant lampriforms.

The divisions between the frontals and other bones are not prominent externally, and our µCT data are insufficient to resolve most of the sutures between ossifications of the neurocranium (Figs. 7-8). We therefore describe the gross morphology of the neurocranium, drawing attention to divisions between bones when these are visible. Posterior to the incomplete frontal vault, the roof of the skull is complete, and forms the broken base of a probable sagittal crest that extends along the posterior half of the frontal. Posterior to the frontal vault, the roof of the neurocranium is elevated relative to the ethmoid region, giving it a dome-shape appearance in lateral view. The dorsolateral surface of the posterior half of the neurocranium is dominated by the supratemporal fossa. This shallow, triangular depression extends anteriorly to the level of mid-orbit. A fenestra lies in the centre of the supratemporal fossa. Sutures are visible extending from this fenestra. These define the edges of the bones contributing to the supratemporal fossa: the epiotic posterodorsally, the pterotic posterolaterally, the parietal anterodorsally, and the sphenotic anterolaterally. The dorsolateral surface of the epiotic bears a flattened facet for the posttemporal. A low ridge of bone defines the ventrolateral margin of the supratemporal fossa and separates it from the dilatator fossa. The narrow, oval-shaped hyomandibular facet lies ventral to the dilatator fossa and straddles the division between the pterotic and the sphenotic.

Viewed posteriorly, the braincase has a roughly triangular profile dorsal to the foramen magnum (Figs. 4, 7-8). The foramen magnum communicates dorsally with another opening in the back of the skull through a narrow gap between median extensions of the exoccipitals, forming an inverted keyhole-shaped opening. The supraoccipital extends posteroventrally to contribute to the dorsal fringe of this opening, but does not separate the exoccipitals themselves or contribute to the

foramen magnum. The occipital condyle is located approximately at the level of the upper half of the orbit, placing it midway between the base of the neurocranium as defined by the parasphenoid and the dorsal peak of the supraoccipital as preserved. The occipital condyle is broadest dorsally, with large, kidney-shaped facets of the posterior margins of the exoccipitals that extend dorsolaterally to partially define the lateral margins of the foramen magnum. These exoccipital condyles meet on the midline immediately ventral to the foramen magnum, but they are separated ventrally by the basioccipital condyle. This condyle has an angular dorsal margin and rounded ventral margin in posterior view and is roughly the size of a single exoccipital condyle.

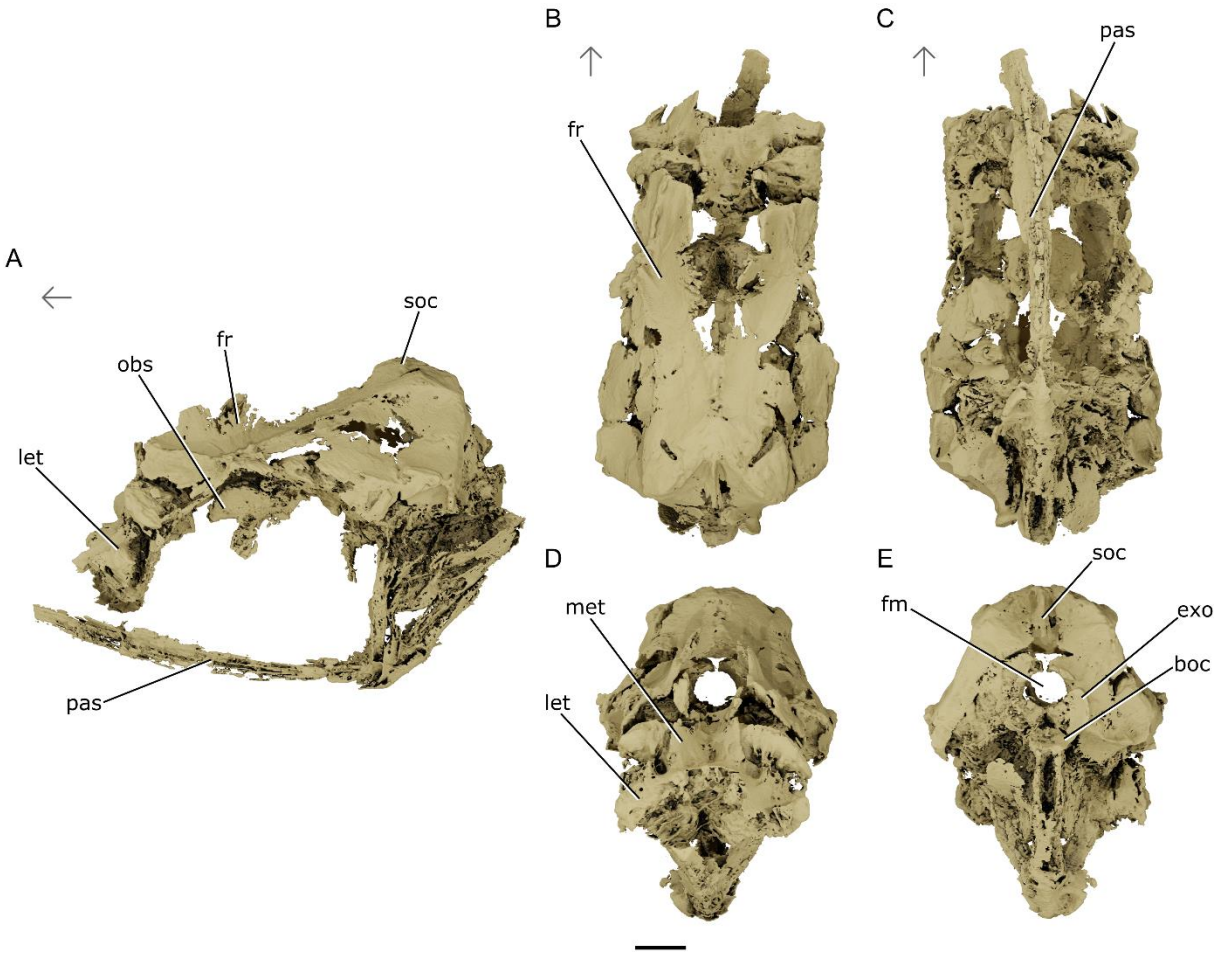

Figure 7. Neurocranium of †*Whitephippus tamensis*. NHMUK PV P 35057, London Clay Formation, early Eocene (Ypresian), Southeast England, UK. Rendered µCT models showing the (**A**) lateral, (**B**) dorsal, (**C**) ventral, (**D**) anterior, and (**E**) posterior views. Abbreviations: **boc**, basioccipital; **exo**, exoccipital; **fm**, foramen magnum; **fr**, frontal; **let**, lateral ethmoid; **met**, mesethmoid; **obs**, orbitosphenoid; **pas**, parasphenoid; **soc**, supraoccipital. Arrows indicate anatomical anterior. Scale bar represents 1 cm.

Divisions between bones contributing to the ventrolateral walls of the otic region are not clear in available material. In posterior view, these walls appear straight, joining ventrally in an acute angle that gives the braincase ventral to the occipital condyle the profile of an inverted triangle. In lateral view, the ventral margin of the otic and occipital regions is strongly sloped, defining an angle of roughly 45° with a line extending from

the main axis of the parasphenoid in the orbital region. The posterior branch of the parasphenoid approaches—but does not contact—the basioccipital condyle. A narrow notch is present in the posterior margin of the parasphenoid. It extends anteriorly roughly one-third to one-half the length of the posterior stalk of the bone. The anterior and posterior portions of the parasphenoid join at a conspicuous angle at the level of the anterior margin of the myodome. The parasphenoid bears two sets of laterodorsal processes in this region, roughly perpendicular with the shaft of the parasphenoid. The more anterior of these is long and narrow, and extends along the anterior margin of the prootic, bracing the slender, rod-like lateral commissure. The posterior projection is shorter, but anteroposteriorly thickened, and is notched by a large foramen in the neurocranium for the internal carotid artery. Anterior to these processes, the parasphenoid widens in ventral view. There is a gap between the parasphenoid and the ethmoid region. We assume this would have been bridged by the vomer in life, but this bone is not preserved in available material.

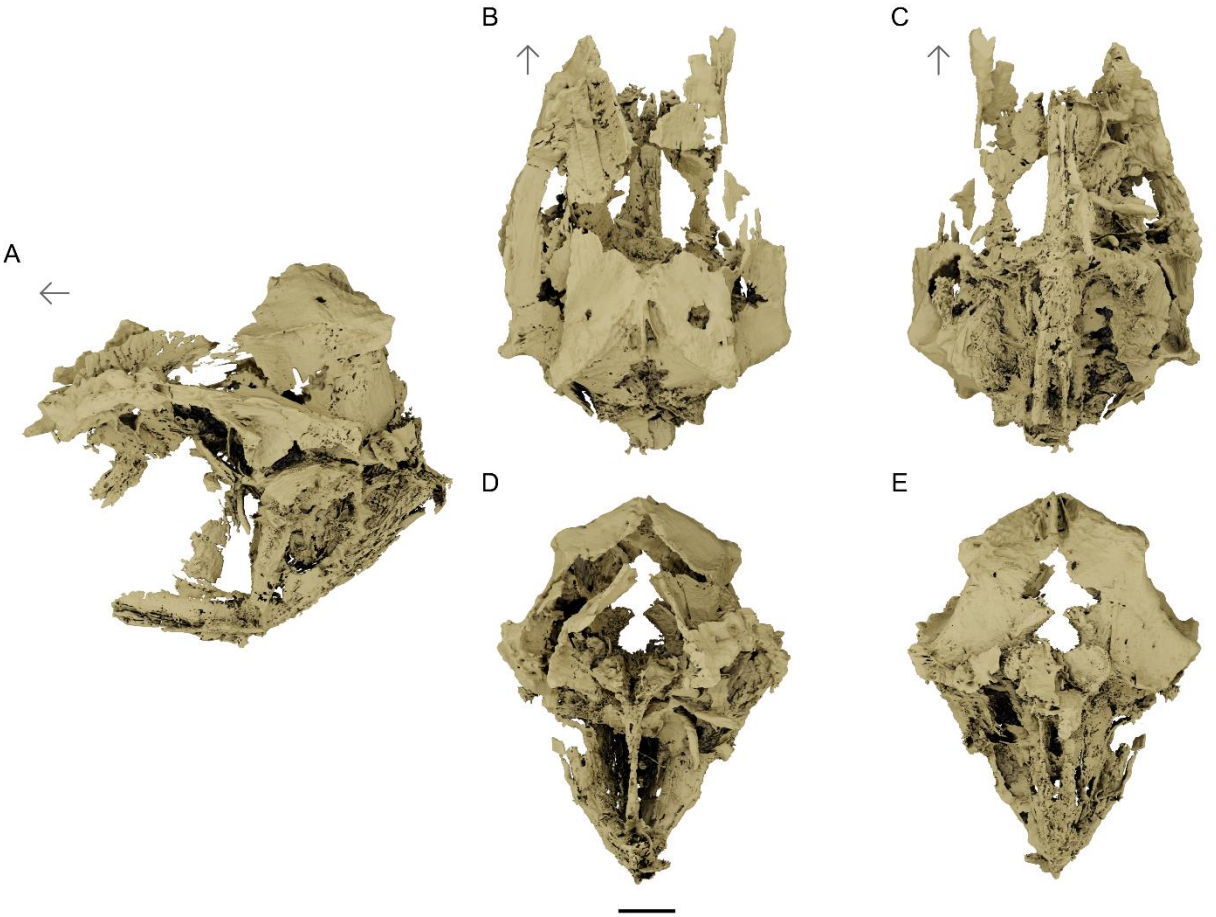

Figure 8. Neurocranium of †*Whitephippus tamensis*. NMS 1864.6.9, London Clay Formation, early Eocene (Ypresian), Southeast England, UK. Rendered µCT models showing the (**A**) lateral, (**B**) dorsal, (**C**) ventral, (**D**) anterior, and (**E**) posterior views. Abbreviations: **boc**, basioccipital; **bsp**, basisphenoid; **exo**, exoccipital; **fm**, foramen magnum; **fr**, frontal; **obs**, orbitosphenoid; **pas**, parasphenoid; **soc**, supraoccipital. Arrows indicate anatomical anterior. Scale bar represents 1 cm.

The median basisphenoid is ‘T’ shaped in anterior view, and completely divides the optic foramen from the myodome. The ventral process of the basisphenoid is long, slender, and directed slightly posteriorly. The ventral portions of the basisphenoid in the NHMUK material are not clearly shown in µCT data, but NMS 1864.6.9 clearly shows a pedicel on the midline of the parasphenoid, reaching dorsally to nearly contact the basisphenoid. These bones were most likely separated by cartilage in life.

The optic foramen is large and situated on the posterdorsal roof of the interorbital region. It is delimited posteroventrally by the basisphenoid, laterally by the paired pterosphenoids, and anteriorly by the median orbitosphenoid. In ventral view, the orbitosphenoid is wider than long. Its posterior margin bears a deep notch where the bone delimits the optic foramen, and its anterior margin is more subtly excavated. The orbitosphenoid carries a pronounced keel along its ventral midline, which is directed at a subtle angle anteriorly and has a rounded ventral extremity.

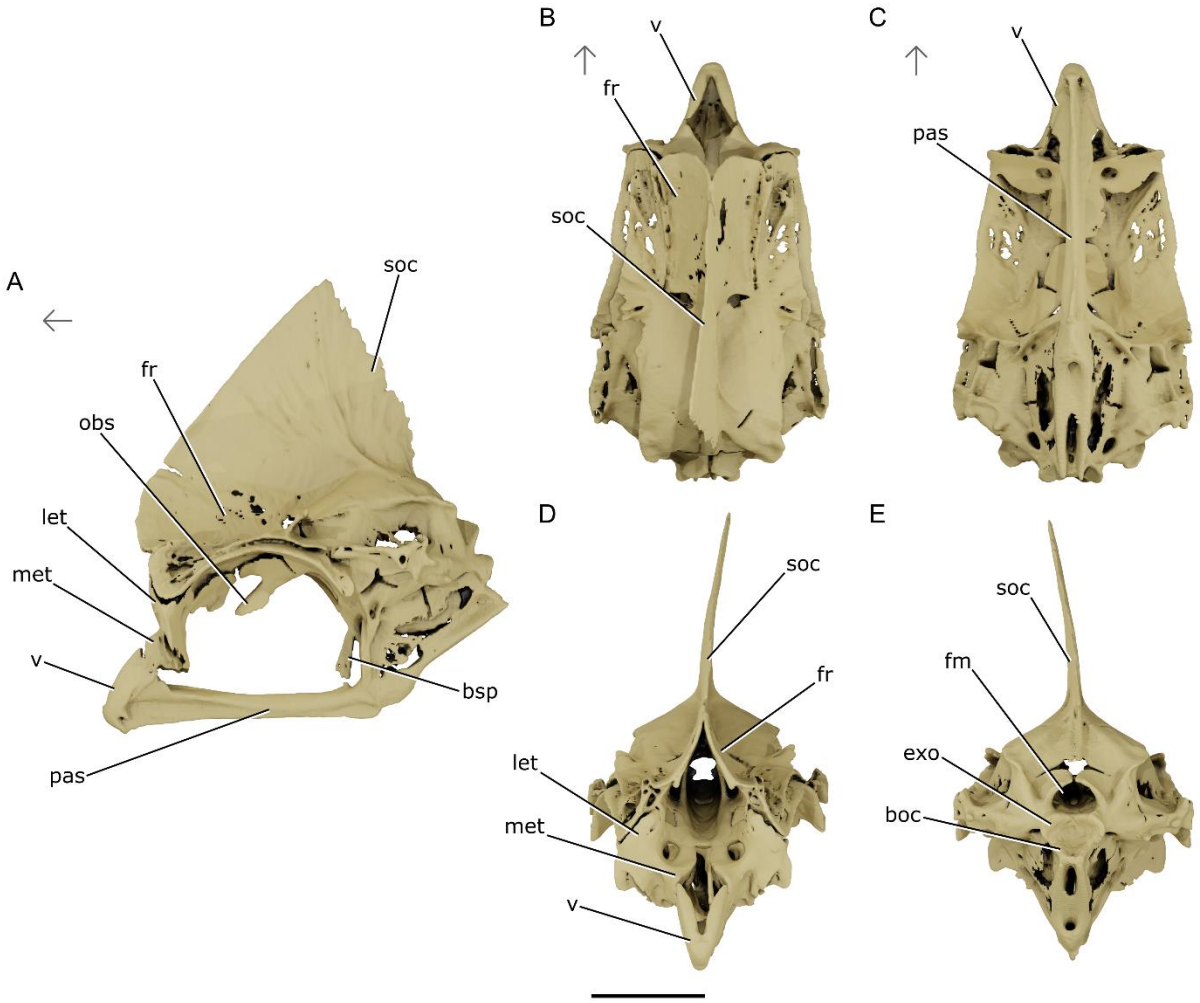

Figure 9. Neurocranium of *Velifer hypselopterus*. UMMZ 220456. Rendered µCT models showing the (**A**) lateral, (**B**) dorsal, (**C**) ventral, (**D**) anterior, and (**E**) posterior views. Abbreviations: **boc**, basioccipital; **bsp**, basisphenoid; **exo**, exoccipital; **fm**, foramen magnum; **fr**, frontal; **let**, lateral ethmoid; **met**, mesethmoid; **obs**, orbitosphenoid; **pas**, parasphenoid; **soc**, supraoccipital; **v**, vomer. Arrows indicate anatomical anterior. Scale bar represents 1 cm.

Infraorbitals, lacrimal and sclerotic ring

The lacrimal (infraorbital 1) is preserved in both NHMUK PV P6479 and PV 35057, but is highly fragmentary in the latter (Figs. 2, 5). It is a plate-like bone with a long anteroposterior axis. The bone is deepest posteriorly, and tapers to a rounded anterior apex. A process extends from the dorsal margin of the bone and bears a concave medial facet that articulates with the lateral ethmoid. The more posterior infraorbitals are not preserved.

Well-developed sclerotic ossicles are present in NHMUK PV P6479, where they are preserved as three fragments (Fig. 1).

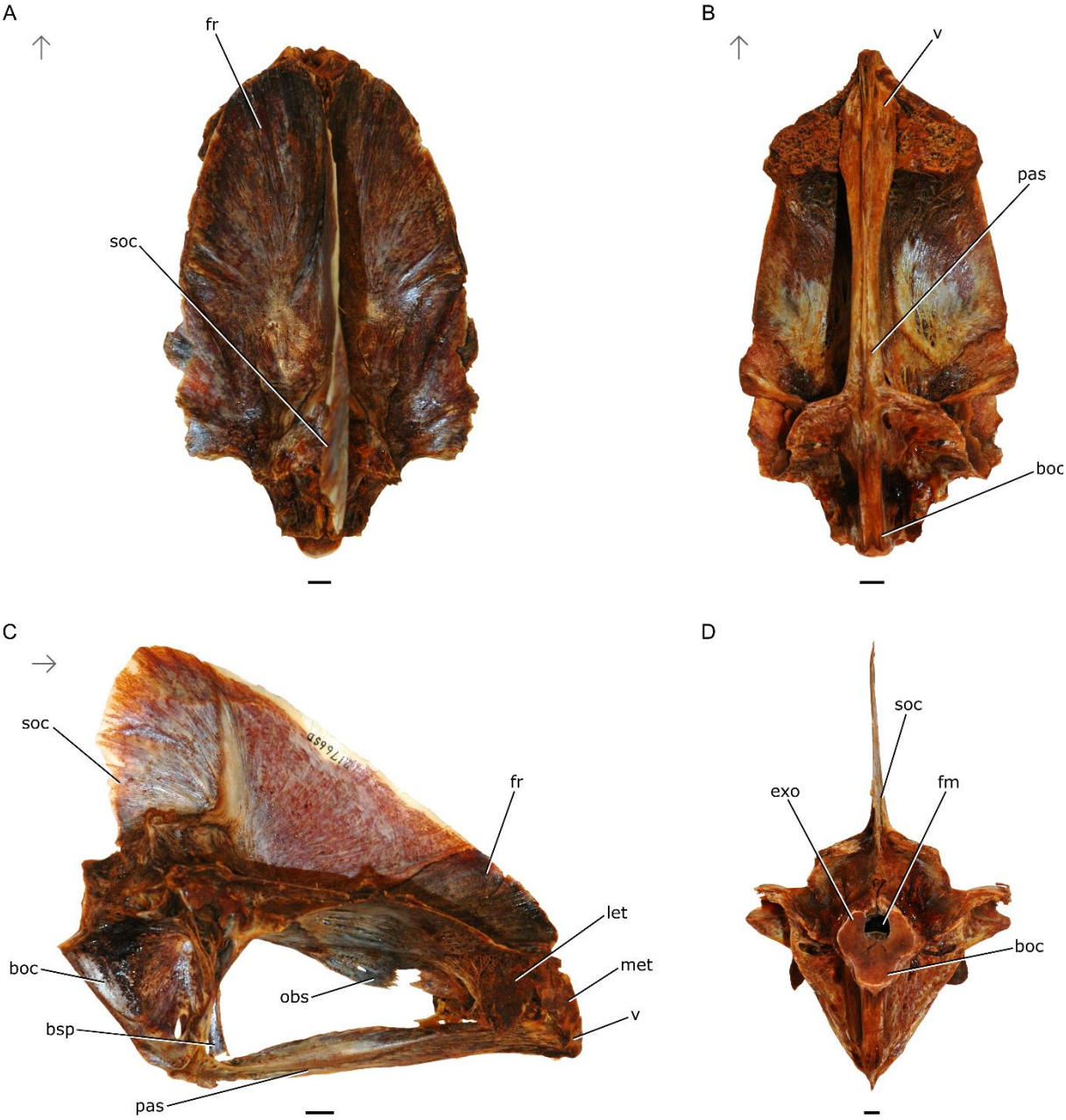

Figure 10. Neurocranium of *Lampris guttatus*. AMNH 79669SD. Photographs showing the (**A**) dorsal, (**B**) ventral, (**C**) lateral, and (**D**) posterior views. Abbreviations: **boc**, basioccipital; **bsp**, basisphenoid; **exo**, exoccipital; **fm**, foramen magnum; **fr**, frontal; **let**, lateral ethmoid; **met**, mesethmoid; **obs**, orbitosphenoid; **pas**, parasphenoid; **soc**, supraoccipital; **v**, vomer. Arrows indicate anatomical anterior. Scale bars represent 1 cm.

Jaws

The jaws are partially preserved in NHMUK PV P6479 and PV 35057 (Figs. 1-2, 5). The anguloarticular is high and triangular shaped, being much narrower near its articulation with the quadrate than at its contact with the dentary. A posteriorly oriented prong extends from the bone ventral to the glenoid. A narrow gap separates the dentary from the anguloarticular. There is no autogenous retroarticular ossification. The dentary is incomplete in all available specimens. Its posterior portion shows a straight dorsal margin, with no visible teeth.

The upper jaws are partially preserved in NHMUK PV P6479 but are absent altogether in PV 35057. They appear to be much smaller than the high and deep lower jaws. The maxilla is toothless and anteroposteriorly elongate. Its posterior extremity is slightly rounded and it curves dorsally at its anterior end.

The ascending processes of the premaxillae are preserved in NHMUK PV P6479. They are closely associated together throughout their length. A bulbous pyritic mass lies between the ascending processes and protrudes anteriorly. This may correspond to a mineralized rostral cartilage, as Casier (1966) proposed. Apart from the ascending processes, no other parts of the premaxillae are visible due to a combination of breakage and concealment by overlying matrix and the maxillae.

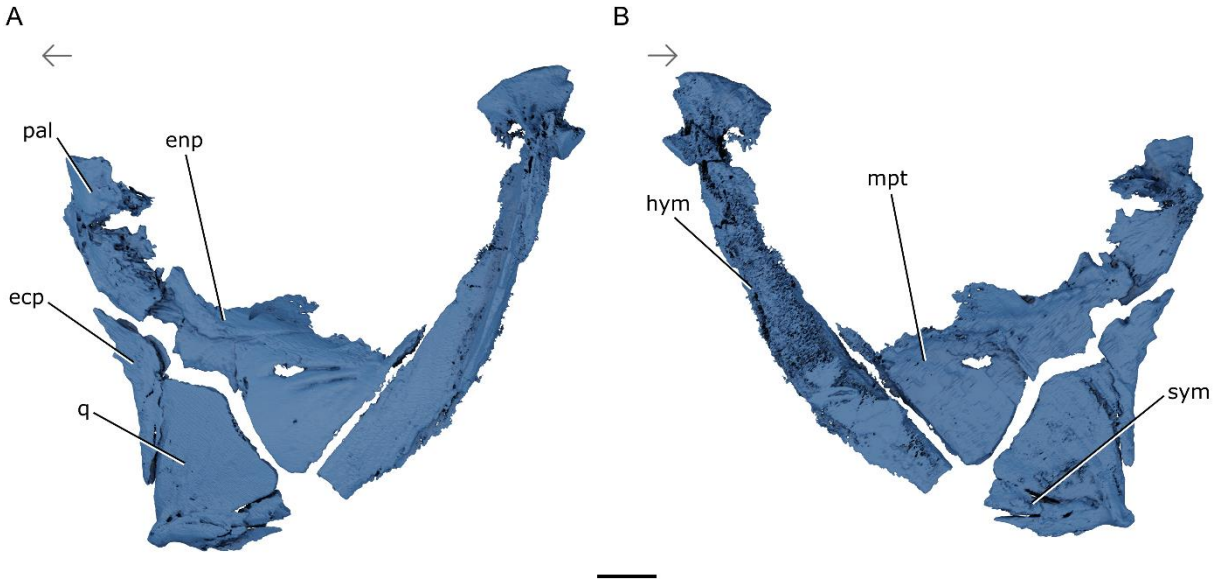

Figure 11. Left suspensorium of †*Whitephippus tamensis*. NHMUK PV P 35057, London Clay Formation, early Eocene (Ypresian), Southeast England, UK. Rendered µCT models showing the left suspensorium in (**A**) lateral and (**B**) mesial views. Abbreviations: **ecp**, ectopterygoid; **enp**, endopterygoid; **hym**, hyomandibula; **mpt**, metapterygoid; **pal**, palatine; **q**, quadrate; **sym**, symplectic. Arrows indicate anatomical anterior. Scale bar represents 1 cm.

Suspensorium

A complete suspensorium is preserved in NHMUK PV 35057 (Fig. 11). Only its ventral portion is visible externally, but concealed regions are clear in the µCT reconstructions.

The hyomandibula is very long and its ventral shaft is especially well developed. Its articular head is relatively narrow and directed slightly anteriorly at the level of its contact with the neurocranium. This zone of contact consists of a single condyle, slightly pinched laterally in its middle. Posteroventral to the articular head, a short condyle contacts the opercular bone, projecting slightly ventrally. A conspicuous lateral ridge extends from the articular head near or along the posterior edge of the ventral

shaft of the hyomandibula. This ridge is approximately two-thirds the length of the entire ventral shaft and delimits an anteriorly-oriented fossa bounded by the anterior lamina of the ventral shaft of the hyomandibula. A narrow posterior lamina is restricted to the region immediately ventral to the opercular condyle of the hyomandibula and is completely covered by the preopercle. Anterior and ventral to the ridge, the surface of the hyomandibula is flat and faces laterally. Overall, the ventral shaft of the hyomandibula is strap-shaped, with a gentle convexity to its posterior margin. The ventral shaft is widest at the level of the dorsal articulation of the metapterygoid and terminates distally at a blunt tip, although this may be a taphonomic break.

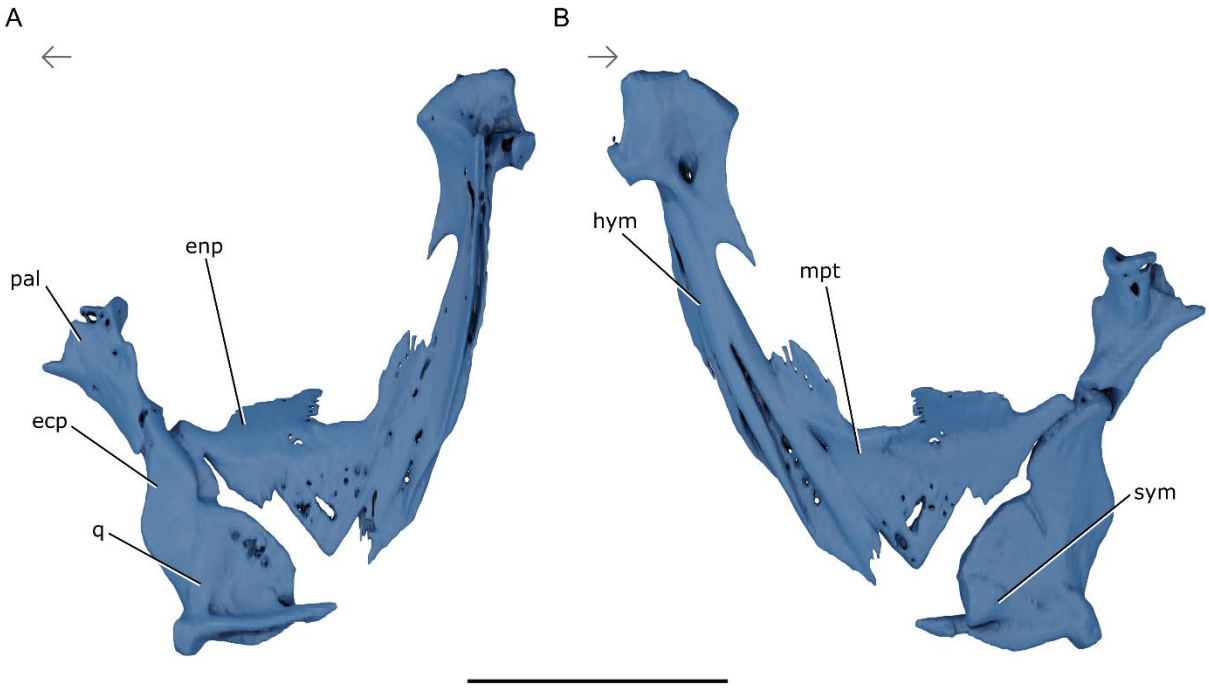

Figure 12. Left suspensorium of *Velifer hypselopterus*. UMMZ 220456. Rendered µCT models showing the left suspensorium in (**A**) lateral and (**B**) mesial views. Abbreviations: **ecp**, ectopterygoid; **enp**, endopterygoid; **hym**, hyomandibula; **mpt**, metapterygoid; **pal**, palatine; **q**, quadrate; **sym**, symplectic. Arrows indicate anatomical anterior. Scale bar represents 1 cm.

The metapterygoid is a laminar bone that is roughly triangular in shape. The entire posterior edge of the bone contacts the anterior margin of the ventral shaft of the hyomandibula. The metapterygoid bears a posteriorly directed, spur-like process that extends from the posterodorsal corner of the bone, tracing the anterior margin of the hyomandibula. The surface of the metapterygoid faces laterally, but folds slightly along its dorsal edge.

The quadrate is subtriangular, with its tip forming a ventrally projecting condyle that articulates with the glenoid fossa of the anguloarticular. The posteroventral edge of the bone bears a thickening aligned with the quadrate condyle. The short symplectic rests in a notch that is aligned with this thickened ridge at the posterodorsal corner of the quadrate. The anterior margin of the quadrate bears a faint, laterally directed furrow at its contact with the ectopterygoid and anguloarticular. The dorsal margin of the bone comprises two edges, the more anterior of which forms a margin with the ectopterygoid, while the more posterior traces the profile of the anteroventral margin of the metapterygoid. In NHMUK PV 35057, the left quadrate is in life position, but the right one is displaced and upturned.

The endopterygoid is triradiate, with anterior, posterior and ventrolateral rami. The posterior and ventrolateral branches of the bone embrace the anterior angle of the metapterygoid. The flat surface of the posterior ramus shows a strong dorsomedial orientation. The anterior ramus bears a longitudinal ridge at its dorsal margin, presumably to strengthen the articulation with the ectopterygoid.

The anterior margin of the suspensorium is defined by the ectopterygoid and palatine. The ectopterygoid is slightly crescentic. Its posteroventral ramus is longer, narrower and more tapered than its anterior ramus; the two rami form a moderately concave ventral margin. The dorsal margin is more strongly pronounced and the mesial margin of the bone is slightly concave. The palatine is subrectangular. It contacts the ectopterygoid and endopterygoid posteriorly, and the braincase at the level of the lateral ethmoids anteriorly. There is no distinct palatine prong marking the articulation between the suspensorium and the upper jaw. However, the connection between the palatine and the braincase is marked by an anterodorsally directed articular head.

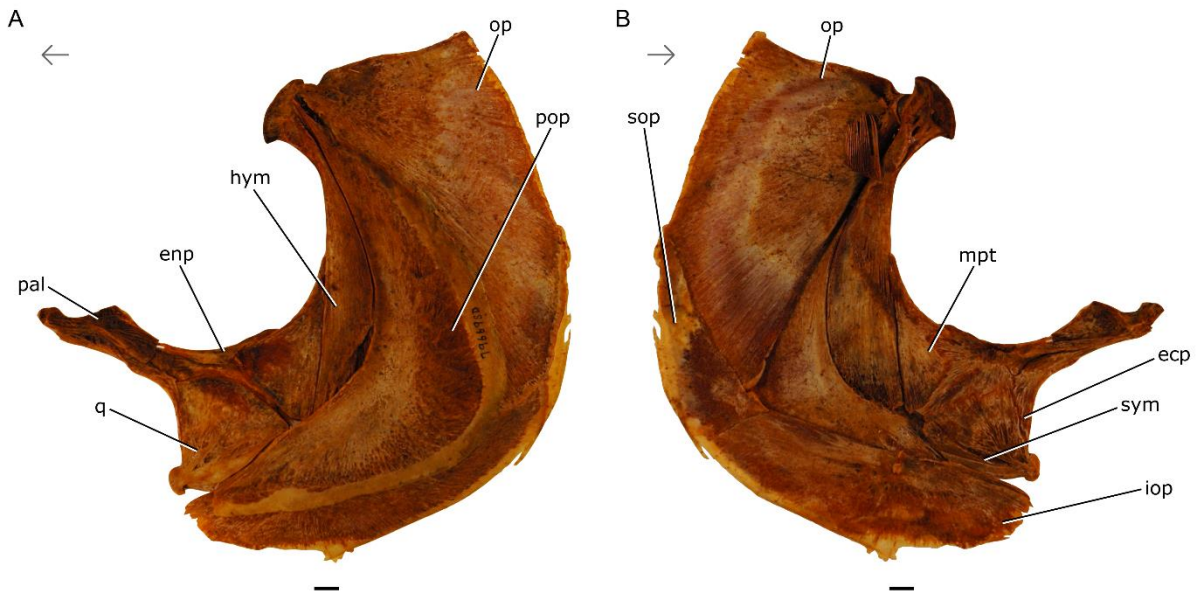

Figure 13. Left suspensorium of *Lampris guttatus*. AMNH 79669SD. Photographs showing the left suspensorium in (**A**) lateral and (**B**) mesial views. Abbreviations: **ecp**, ectopterygoid; **enp**, endopterygoid; **hym**, hyomandibula; **iop**, interopercle; **mpt**, metapterygoid; **op**, opercles; **pal**, palatine; **pop**, preopercle; **q**, quadrate; **sop**, subopercle; **sym**, symplectic. Arrows indicate anatomical anterior. Scale bars represent 1 cm.

Opercular series

Apart from the isolated braincase of NHMUK PV 41384, all specimens of †*Whitephippus* preserve portions of the opercle and preopercle (Figs. 1-3, 5-6). Portions of the interopercle are preserved in NHMUK PV P6479, where the bone is visible along the posteroventral margin of the preopercle. The opercle is deep, nearly reaching the ventral margin of the hyomandibular shaft. The anterior margin of the opercle is nearly vertical, while the dorsal margin is gently angled with its dorsal apex located at the posterior margin of the bone. The posterior margin of the bone is gently convex, and the opercle terminates ventrally in a blunt tip. The facet for the hyomandibula is located at the junction of the dorsal and anterior margins of the opercle and is produced as an anterodorsally extending projection in lateral view.

The apex of the dorsal limb of the preopercle is located immediately ventral to the articulation between the opercle and hyomandibula. The preopercle is crescent shaped, and the dorsal limb is substantially longer than the ventral one. At their extremities, these two limbs are oriented approximately perpendicular to one another.

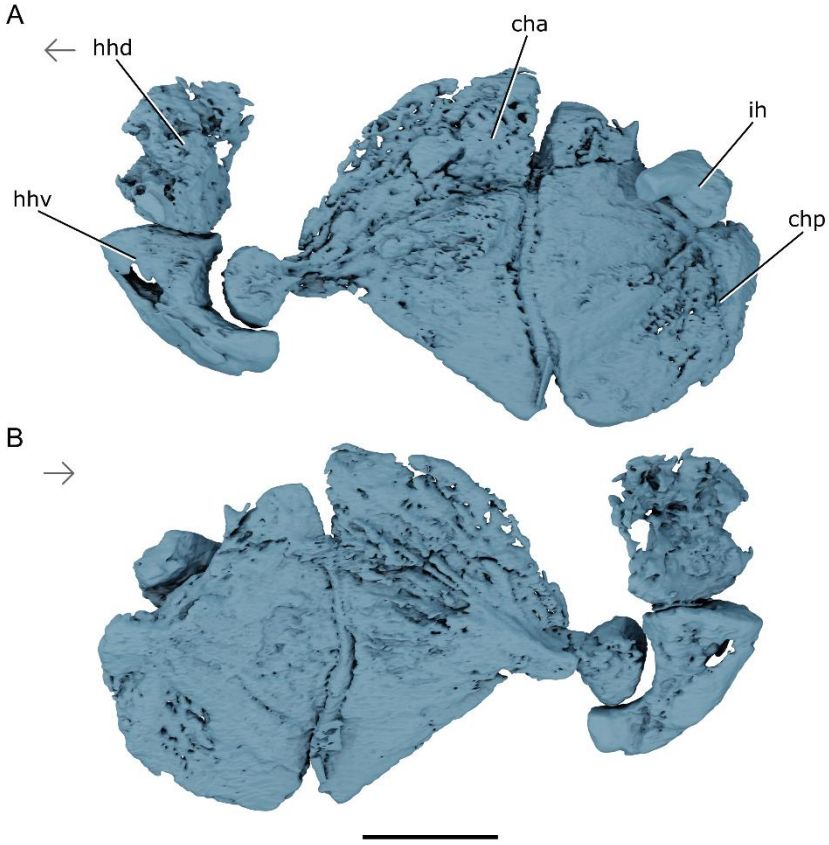

Figure 14. Left ventral hyoid of †*Whitephippus tamensis*. NHMUK PV P 35057, London Clay Formation, early Eocene (Ypresian), Southeast England, UK. Rendered µCT models showing the (**A**) lateral and (**B**) mesial views of the hypohyals, ceratohyals, and interhyal. Abbreviations: **cha**, anterior ceratohyal; **chp**, posterior ceratohyal; **hhd**, dorsal hypohyal; **hhv**, ventral hypohyal; **ih**, interhyal. Arrows indicate anatomical anterior. Scale bar represents 1 cm. Urohyal not imaged.

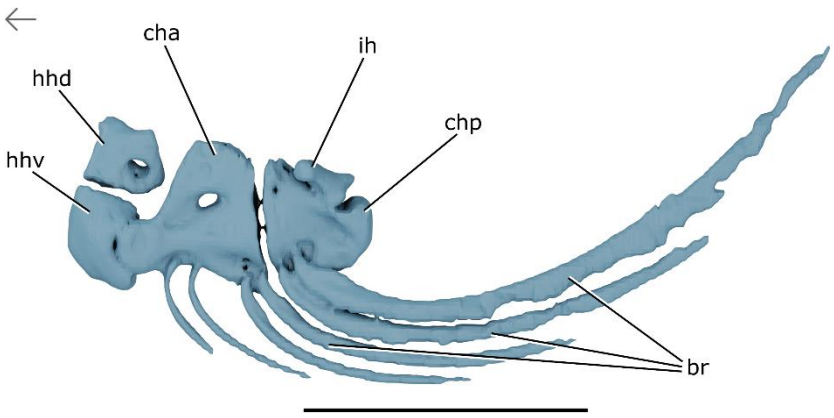

Figure 15. Left ventral hyoid of *Velifer hypselopterus*. UMMZ 220456. Rendered µCT model showing the anterior axial elements in right lateral view. Abbreviations: **br**, branchiostegals; **cha**, anterior ceratohyal; **chp**, posterior ceratohyal; **hhd**, dorsal hypohyal; **hhv**, ventral hypohyal; **ih**, interhyal. Arrow indicates anatomical anterior. Scale bar represents 1 cm. Urohyal not imaged.

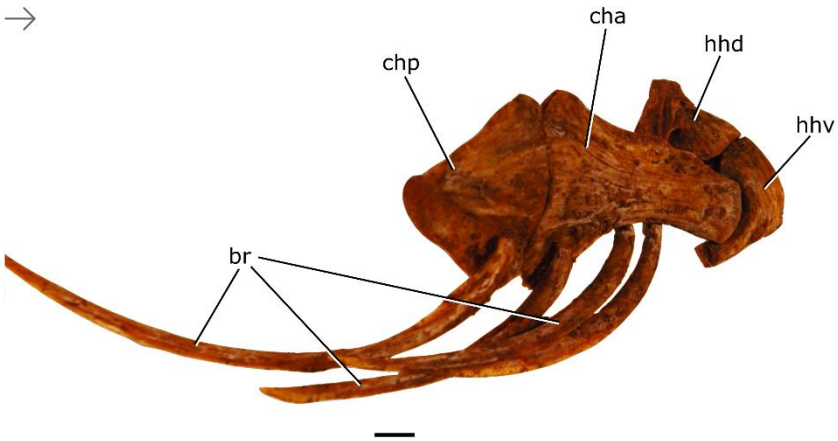

Figure 16. Right ventral hyoid of *Lampris guttatus* AMNH_ 79669SD. Photograph showing the anterior ventral hyoid in right lateral view. Abbreviations: **br**, branchiostegals; **cha**, anterior ceratohyal; **chp**, posterior ceratohyal; **hhd**, dorsal hypohyal; **hhv**, ventral hypohyal. Arrow indicates anatomical anterior. Scale bar represents 1 cm. Urohyal not imaged.

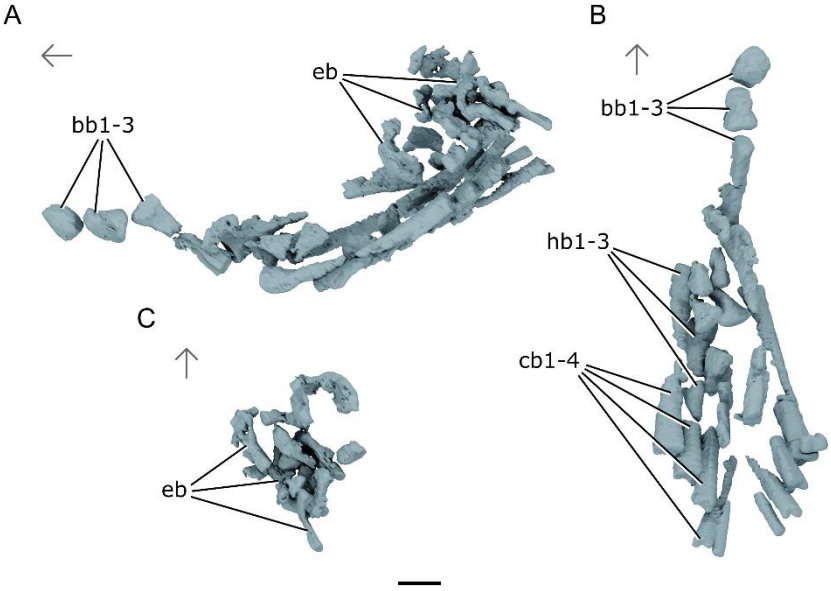

Figure 17. Gill skeleton of †*Whitephippus tamensis*. NHMUK PV P 35057, London Clay Formation, early Eocene (Ypresian), Southeast England, UK. Rendered µCT models showing the (**A**) complete gill skeleton in lateral view, (**B**) the ventral gill skeleton in dorsal view, and (**C**) the dorsal gill skeleton in ventral view. Abbreviations: **bb**, basibranchials; **cb**, ceratobranchials; **eb**, epibranchials; **hb**, hypobranchials. Arrows indicate anatomical anterior. Scale bar represents 1 cm.

Branchial skeleton and ventral hyoid arch

The ventral hyoid arch and branchial skeleton are concealed in all specimens but are visible in tomograms of NHMUK PV 35057 (Figs. 14, 17). The anterior and posterior ceratohyals are similar in size, and join one another along a subvertical junction. There is no obvious suturing between the two bones, and together they form a lozenge-shaped structure. There is no visible foramen in the anterior ceratohyal. The posterior ceratohyal is an obtuse trapezoid in lateral view and bears a fossa on its posterodorsal margin onto which the interhyal articulates. The interhyal is hooked, such that the larger ventral margin is in contact with the posterior ceratohyal—with the most dorsal point being at the midsection of the element—before curving laterally to form a small articular head with the symplectic. The anterior ceratohyal tapers anteriorly, forming a well-developed articular head situated at the tip of a short process. This condyle articulates with a deep cavity in the posterior margin of the ventral hypohyal. This posterior excavation gives the ventral hypohyal a hook-shaped profile in lateral view. Dorsally, the ventral hypohyal articulates with a nodular, dorsal hypohyal. There is no suturing between these bones, and the displacement of the dorsal hypohyals suggests the articulation between the hypohyals was cartilaginous. The shape of the posterior margin of the dorsal hypohyal corresponds to the anterodorsal margin of the anterior ceratohyal. This, combined with the presence of a

clear joint between the hypohyals and ceratohyals, suggests the potential for flexion within the ventral hyoid arch.

A combination of incomplete ossification and displacement of bones makes interpretation of the branchial skeleton complicated (Fig. 17), so our description is abbreviated. Five rod-like ceratobranchials are preserved. The first four ceratobranchials are relatively robust and grooved ventrally, while the fifth ceratobranchial is conspicuously more gracile, and consists of a slender rod without a groove. There are three basibranchials.

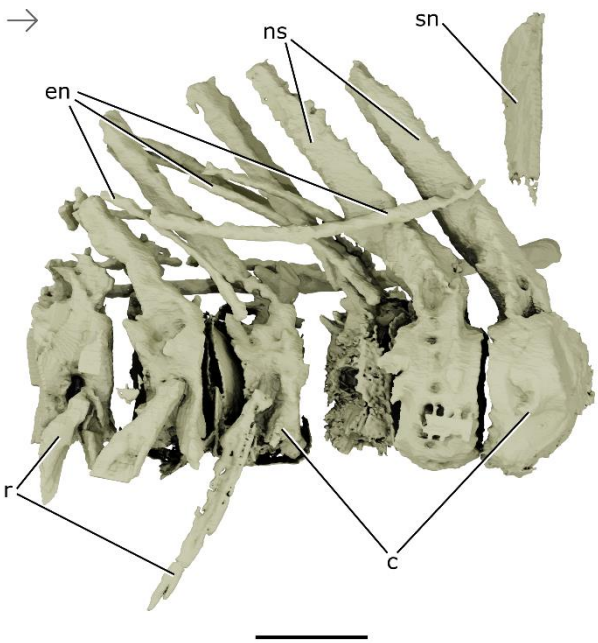

Figure 18. Vertebral elements of †*Whitephippus tamensis* in left lateral view. NMS 1864.6.9, London Clay Formation, early Eocene (Ypresian), Southeast England, UK. Rendered µCT model showing the vertebral elements in right lateral view. Abbreviations: **c**, centra; **en**, epineurals; **ns**, neural spines; **r**, ribs; **sn**, supraneural. Arrow indicates anatomical anterior. Scale bar represents 1 cm.

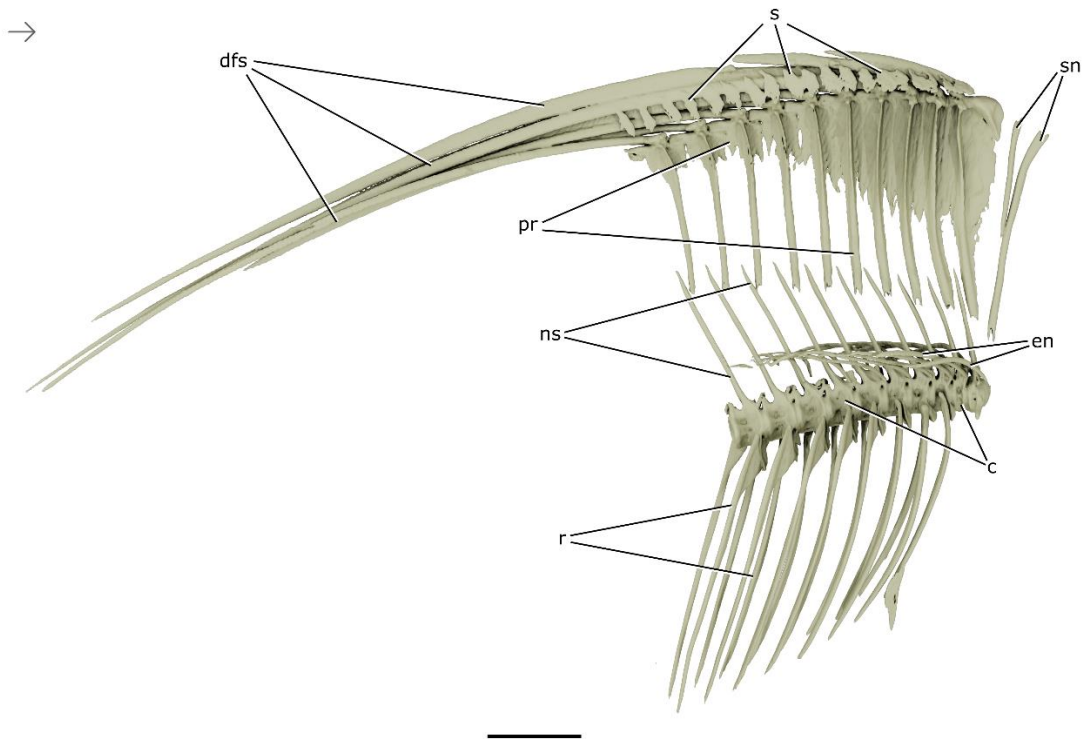

Figure 19. Anterior axial skeleton of *Velifer hypselopterus* in left lateral view. UMMZ 220456. Rendered µCT model showing the anterior axial elements in right lateral view. Abbreviations: **c**, centra; **dfs**, dorsal fin spines; **en**, epineurals; **ns**, neural spines; **pr**, proximal radials of the dorsal fin; **r**, ribs; **s**, scales; **sn**, supraneural. Arrow indicates anatomical anterior. Scale bar represents 1 cm.

Vertebral column and dorsal fin

Six complete vertebrae are visible in tomograms of NMS 1864.6.9 (Fig. 18). The neural spines form the neural arches ventrally and are unpaired distally. The neural spines are straight and angled posteriorly. There are a series of epineurals contacting the neural spines on the first two vertebrae, and the base of the neural arches on vertebrae 3–6. The preserved ribs are slender and are visibly angled. Their articular heads directly contact the vertebrae at the level of their centra. The vertebral centra bear no parapophyses or haemal arches. A straight, rod-like bone lays at an oblique angle anterior to the most anterior neural spine. We interpret it as the ventral extremity of a single supraneural. No other supraneural is visible—though it is unclear if this is taphonomic or biological. No dorsal-fin pterygiophores are visible, presumably because their ventral extremities were dorsal to the area that is preserved in the specimen.

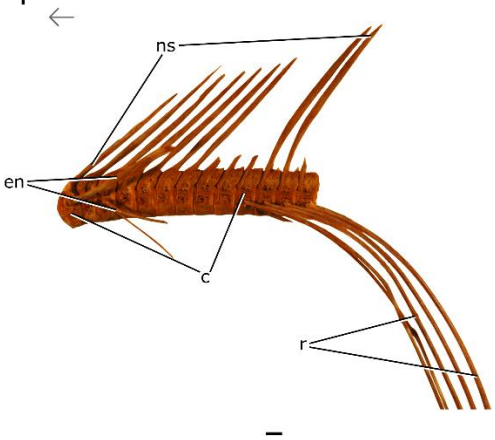

Figure 20. Anterior axial skeleton of *Lampris guttatus* in left lateral view. AMNH 79669SD. Photograph showing the anterior axial elements in right lateral view. Abbreviations: **c**, centra; **en**, epineurals; **ns**, neural spines; **r**, ribs. Arrow indicates anatomical anterior. Scale bar represents 1 cm.

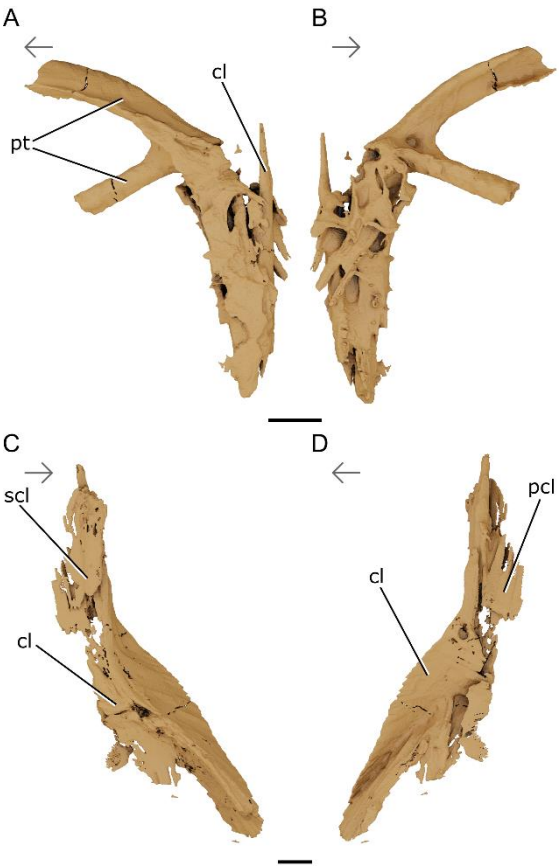

Figure 21. Pectoral girdle of †*Whitephippus tamensis*. NMS 1864.6.9, London Clay Formation, early Eocene (Ypresian), Southeast England, UK. Rendered µCT models showing the (**A**) lateral and (**B**) mesial views of the left dorsal pectoral girdle elements, and the (**C**) lateral and (**D**) mesial views of the right ventral pectoral girdle elements. Abbreviations: **cl**, cleithrum; **pcl**, postcleithrum; **pt**, posttemporal; **scl**, supracleithrum. Arrows indicate anatomical anterior. Scale bars represent 1 cm.

Pectoral girdle and fin

NMS 1864.6.9 best preserves the dorsal portions of the pectoral girdle on the left side of the specimen, while the ventral portions of the pectoral girdle are best preserved on the right (Fig. 21). The dorsal and ventral branches of the posttemporal extend the length of three vertebrae. The dorsal branch ends in a broad, flat head that articulates with the epioccipital. The ventral branch ends in a cylindrical head that articulates with the intercalar. Tomographic cross-sections of the posttemporal show highly mineralized struts along the long axis of the bone. The

ventrolateral margin of the posttemporal articulates with a shattered supracleithrum whose shape cannot be adequately described. Posterior to the supracleithrum is the dorsal point of the cleithrum, which is sharply pointed and rises to the approximate height of the posttemporal bifurcation. Ventrally, the cleithrum comprises two flanges—one that continues laterally from the more dorsal portion, and another that penetrates mesially and bears an anteriorly-oriented convexity, such that the cleithrum appears as a chevron in coronal cross-section.

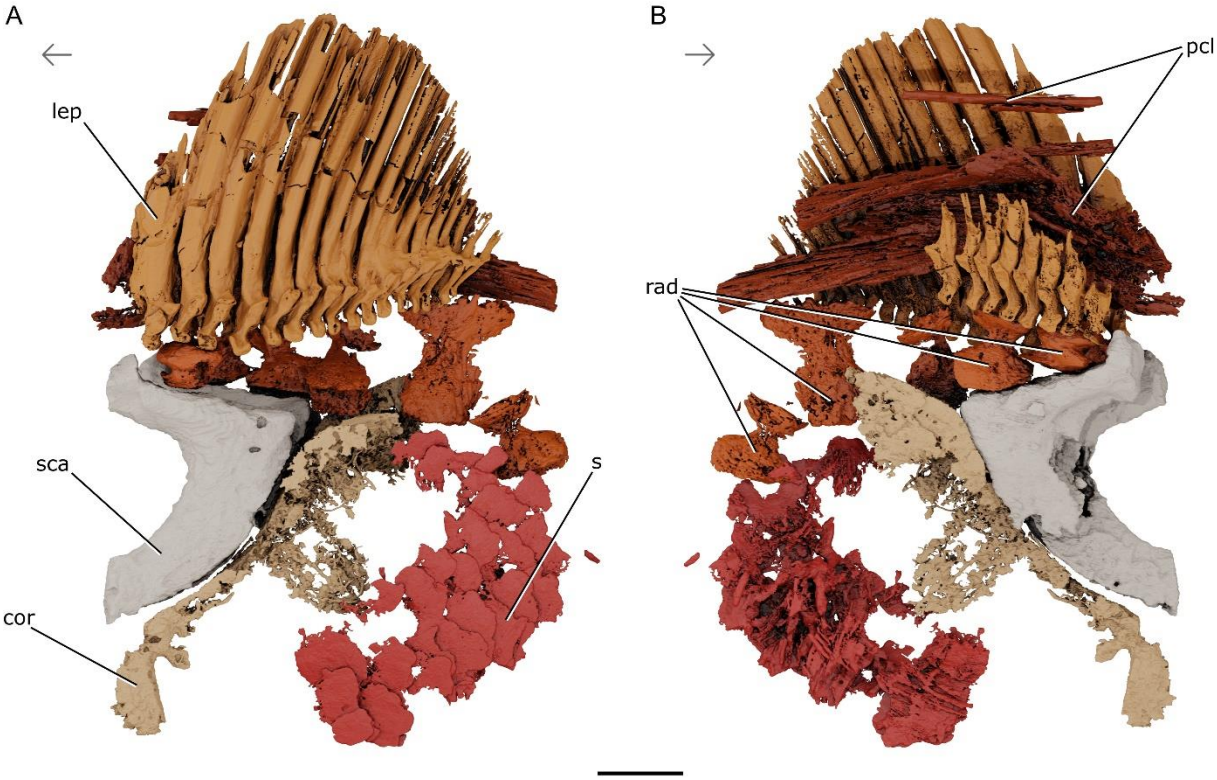

Figure 22. Pectoral fin skeleton of †*Whitephippus tamensis* holotype. NHMUK PV P 6479, London Clay Formation, early Eocene (Ypresian), Southeast England, UK. Rendered µCT models showing the (**A**) left and (**B**) right views of the pectoral fin elements. Abbreviations: **cor**, coracoid; **lep**, lepidotrichia; **pcl**, postcleithrum; **rad**, radials; **s**, scales; **sca**, scapula. Arrows indicate anatomical anterior. Scale bar represents 1 cm.

The pectoral fin is best preserved in NHMUK PV 35057, where the posterior half of the scapula, anterior portions of the coracoid, a complete series of radials, and pectoral fin rays are present (Fig. 22). Additionally, fragments of the postcleithrum are visible between the chondral components of the girdle.

The scapula is broken along the scapular foramen on both the left and right side of the specimen, with a predominantly flat dorsal edge dropping nearly 90° to a swooping margin abutting the coracoid. At the anterodorsal margin of each break is an enlarged knob that forms an embayment for the propterygium (first pectoral radial). The scapular foramen appears to have been exceedingly large relative to the remainder of the pectoral skeleton: its diameter is more than half the height of the scapula. The coracoids are poorly preserved, with only the most dorsal portions articulated well enough to figure. The concave dorsal margin of the coracoid follows the convex ventral margin of the scapula, and its posterior border is similarly a continuation of the posterior border of the scapula.

The radials are displaced, making their identity difficult to ascertain. Despite this, four independent sizes of radials are evident, suggesting that there were four pairs in life. They appear to have extended posteroventrally past the margin of the scapulocoracoidal boundary, such that they would have sat along the cartilage between the scapula and coracoid in life. The anteriormost pectoral radial is stout—reaching a height less than half that of the fourth pectoral radial—and possesses a perforation common to actinopterygians, which confirms its identity as the first pectoral radial. The remaining pectoral radials are approximately hourglass shaped and increase in size across the series—though taphonomic displacement from life position has moved a central radial posterior to the fourth (last) radial on the right side of the pectoral skeleton (Fig. 22, B).

Pectoral fin rays (lepidotrichia) begin at the most anterior boundary of the first pectoral radial and span the length of where the four radials would have sat in life. Each fin ray bears a club-like articular head proximally that attenuates distally before thickening at the junction of the paired lepidotrichia.

Portions of the postcleithrum are visible mesial to the pectoral fin rays, and whether it formed one or two separate ossifications in life is unclear. They are anteroposteriorly elongate at their dorsal extremities and the ventral portions of the postcleithral shaft approximate a triangle in coronal cross-section.

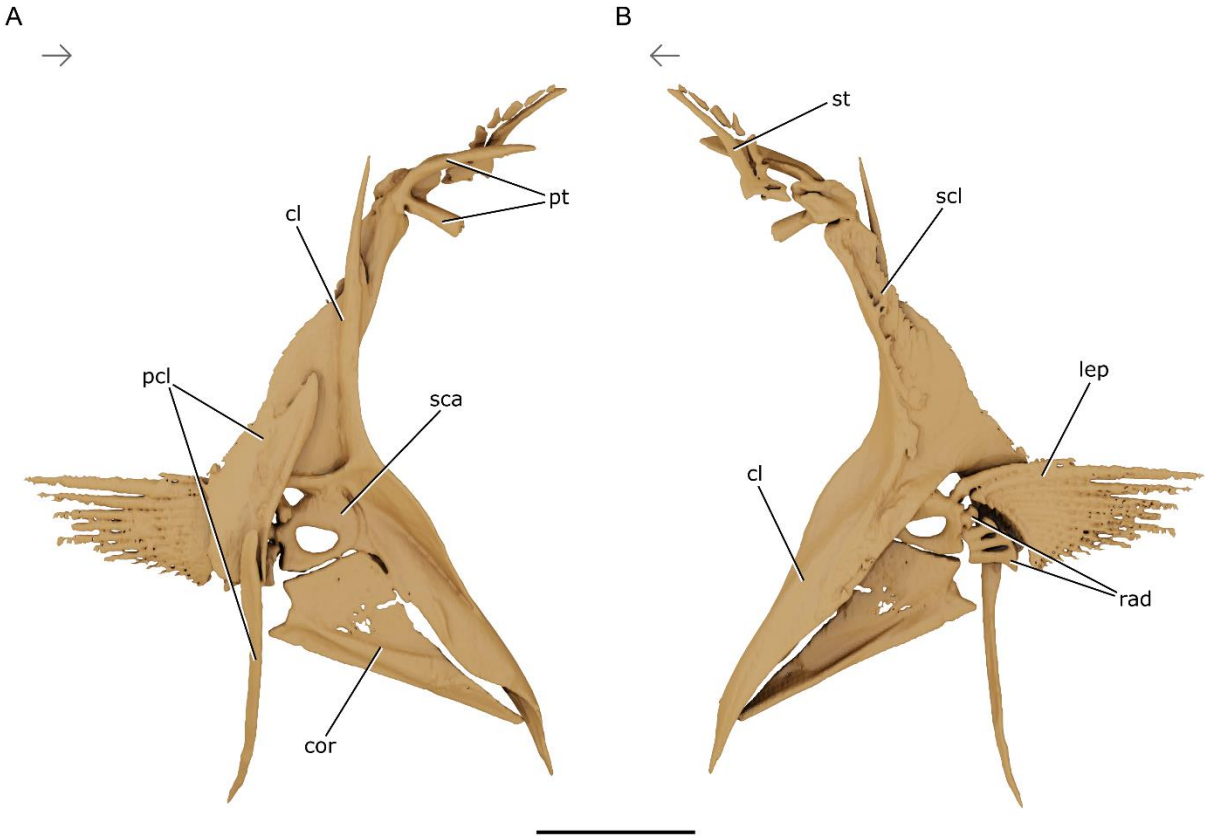

Figure 23. Left pectoral skeleton of *Velifer hypselopterus*. UMMZ 220456. Rendered µCT models showing the (**A**) mesial and (**B**) lateral views of the pectoral skeleton. Abbreviations: **cl**, cleithrum; **cor**, coracoid; **lep**, lepidotrichia; **pcl**, postcleithrum; **pt**, posttemporal; **rad**, radials; **sca**, scapula; **scl**, supracleithrum; **st**, supratemporal. Arrows indicate anatomical anterior. Scale bar represents 1 cm.

Squamation

Squamation is preserved over the pectoral girdle of NHMUK PV P 6479 (Figs. 1, 22), and posterior to the skull of NMS 1864.6.9 (Fig. 3). In both cases the scales are large, slightly overlapping cycloid scales.

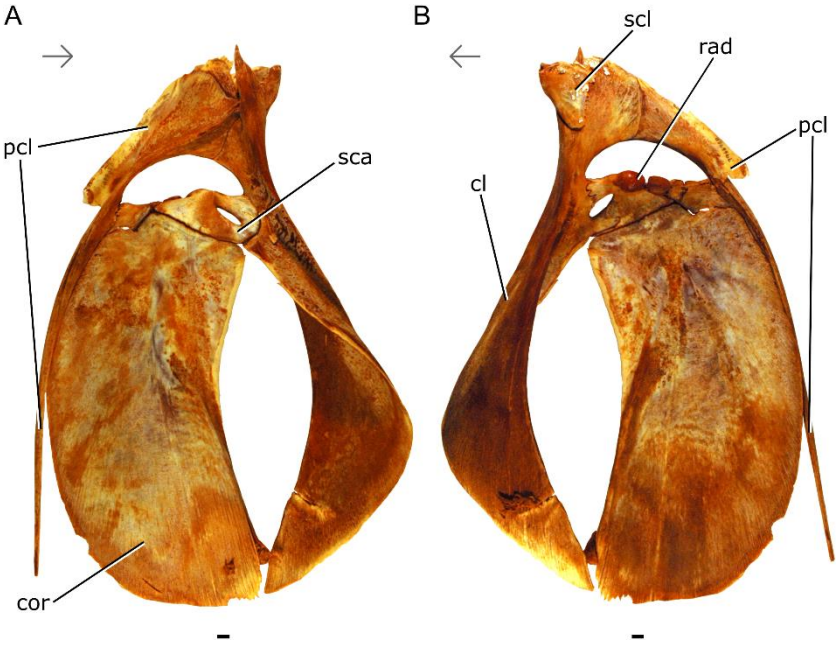

Figure 24. Left pectoral skeleton of *Lampris guttatus*. AMNH 79669SD. Photographs showing the (**A**) mesial and (**B**) lateral views of the pectoral skeleton. Abbreviations: **cl**, cleithrum; **cor**, coracoid; **pcl**, postcleithrum; **rad**, radials; **sca**, scapula; **scl**, supracleithrum. Arrows indicate anatomical anterior. Scale bars represent 1 cm.

DISCUSSION

†*Whitephippus* as a lampriform

Anatomical studies strongly support lampriform monophyly (Davesne et al., 2014, 2016; Delbarre, Davesne, & Friedman, 2016; Oelschläger, 1983; Olney, Johnson, & Baldwin, 1993; Wiley, Johnson, & Dimmick, 1998) with a series of morphological characters that, although not necessarily unique to the clade, are diagnostic when found in combination (Figs. 9-10, 12-13, 15-16, 19-20, 23-24). The lampriform characters found in †*Whitephippus* include: (1) the frontals forming an anterior cavity or 'vault' (Figs. 7, 9-10), (2) the frontals constituting the anterior portion of the sagittal crest (Figs. 7-10), (3) the median ethmoid partially posterior to the lateral ethmoids (Figs. 7, 9-10), (4) the palatine lacking an anterior process that articulates with the upper jaw (Figs. 11-13), and (5) the condylar anterior extremity of the anterior ceratohyal (Figs. 14-16). Moreover, †*Whitephippus* shows characters states that are plesiomorphic for acanthomorphs as a whole and differing in other clades such as percomorphs (including ephippids, to which it was formerly aligned). These include the single-headed condyle of the hyomandibula (Figs. 11-13), the presence of an orbitosphenoid and the supraoccipital not contributing to the dorsal roof of the foramen magnum (Davesne et al., 2016; Johnson & Patterson, 1993; Olney et al., 1993). The attribution of †*Whitephippus* to Lampriformes is then strongly supported by the available anatomical information, in contradiction with Casier's (1966) interpretation as an ephippid.

Position within Lampriformes

Lampriform intrarelationships are largely congruent between phylogenetic studies based on morphological characters: *Lampris* forms a clade with the elongate Taeniosomi, to the exclusion of veliferids (Davesne et al., 2014, 2016; Delbarre et al., 2016; Olney et al., 1993; Wiley et al., 1998). Available evidence suggests that †*Whitephippus* is associated with this nested lampriform group.

The *Lampris* + Taeniosomi clade is notably characterised by a pectoral fin inserting horizontally and supported by three autogenous radials (Fig. 24), the anterior-most being fused to the scapula (Olney et al., 1993). The pectoral fin of †*Whitephippus* inserts horizontally in the only specimen that preserves it (Fig. 1). However, the anterior-most pectoral-fin radial is not fused to the scapula (Fig. 22), corresponding to the plesiomorphic lampriform arrangement (Fig. 23). *Lampris* and taeniosomes also lack a dorsal foramen in the ceratohyal (Oelschläger, 1983), with †*Whitephippus* showing this same condition (Fig. 14). In *Lampris* and taeniosomes, the infraorbital series consists in the lacrimal only (Oelschläger, 1983); this is also the case in †*Whitephippus*, but it is possible, although unlikely, that it is due to incomplete preservation. At the same time, typical taeniosome characters (Olney et al., 1993) are lacking in †*Whitephippus*: the neural spines of the anterior vertebrae are not inclined anteriorly (Figs. 18-20), and there is at least one supraneural bone (supraneurals are absent in taeniosomes).

Finally, two anatomical features seemingly unique to the extant *Lampris* are found in †*Whitephippus*: (1) the exoccipital condyles have kidney-shaped posterior facets (Figs. 4, 10) that define the lateral wall of the foramen magnum (Oelschläger, 1983; Olney et al., 1993) and (2) the anterior ribs insert directly on very short or inexistent vertebral parapophyses (Figs. 18, 20) —there are developed parapophyses in veliferids (Fig. 19).

The available †*Whitephippus* material then shows a unique combination of character states, either shared with the *Lampris* + Taeniosomi clade (pectoral fin inserting horizontally, only one bone in the infraorbital series, no foramen in the anterior ceratohyal) or more specifically with *Lampris* (dorsally-expanded exoccipital condyles, lack of parapophyses). This would support that †*Whitephippus* is a member of the *Lampris* + Taeniosomi clade, and possibly an early member of Lampridae. One character however (the anterior-most pectoral-fin radial is not fused to the scapula), contradicts this attribution. The exact phylogenetic position of †*Whitephippus* within lampriformes is therefore best considered uncertain. A comprehensive phylogenetic analysis of the group including its well-preserved and anatomically disparate Palaeogene fossil members—sometimes collectively termed “veliferoids”—is sorely needed.

It is to be noted that the few molecular studies in which veliferids were included tend to support a different set of deep divergences within lampriforms. Analyses of the 12S mtDNA (Wiley et al., 1998), a combination of six mitochondrial and nuclear markers (Grande, Borden, & Smith, 2013), and complete mitogenomes (Wang et al., 2023) have all recovered a *Lampris* + veliferid clade sister to taeniosomes, contradicting morphological analyses. Future discussions of the phylogenetic position of †*Whitephippus* (and fossil lampriforms in general) will need to acknowledge this possible topology.

Lampriform diversity in the Palaeogene

The lampriform lineage extends to the Late Cretaceous, with the †pharmacichthyids of the Cenomanian of Lebanon, the Cenomanian-Campanian †'aipichthyoids' and

†*Nardovelifer* from the Campanian of Italy (Davesne et al., 2014, 2016; Delbarre et al., 2016). However, the oldest members of the lampriform crown group are Cenozoic in age. *Incertae sedis* ('veliferoid', e.g. deep-bodied) lampriforms from Paleocene deposits in Scandinavia: the Danian København Limestone of Denmark and Southern Sweden yields †*Bathysoma* and cf. †*Palaeocentrotus* (Adolfssen, Milàn, & Friedman, 2017; Davis, 1890), with the former genus also known from an erratic boulder of the Thanetian Lellinge Greensand (Bonde & Leal, 2017; Friedman, Andrews, Saad, & El-Sayed, 2023). The fish-bearing horizon of the Danata Formation of Turkmenistan, which appears to correspond to the Paleocene-Eocene boundary, yields †*Danatinia* and †*Turkmene* (Bannikov, 1999; Daniltshenko, 1968). The Ypresian Fur Formation of Denmark yields the enigmatic †*Palaeocentrotus* plus an undescribed, †*Analectis*-like taxon (Bonde, 1966; Bonde, Andersen, Hald, & Jakobsen, 2008). The earliest lampriforms that can be confidently classified within modern families are two veliferids--†*Veronavelifer* and †*Wettonius*--from the late Ypresian of Bolca, Italy (Bannikov, 1990, 2014; Carnevale & Bannikov, 2018; Carnevale, Bannikov, Marramà, Tyler, & Zorzin, 2014) – although Near *et al.* (2013) have argued that †*Turkmene* is a lamprid, without providing a detailed justification. Bolca also yielded two taxa historically described as lampriforms: the enigmatic '*Pegasus*' (Carnevale & Bannikov, 2018; Carnevale et al., 2014) and †*Bajaichthys* (Bannikov, 2014; Sorbini & Bottura, 1988), the latter now regarded as a morphologically unusual zeiform (Davesne, Carnevale, & Friedman, 2017). The Palaeogene lampriform fossil record includes a variety of taeniosomes, all assigned to Lophotidae: †*Eolophotes* from the Lutetian of Georgia (Daniltshenko, 1980), †*Protolophotus* and †*Babelichthys* from the late Eocene of Iran (Arambourg, 1943; Davesne, 2017; Walters, 1957) and †*Oligolophotes* from the early Oligocene of Russia (Bannikov, 1999). These Russian deposits also yield the *incertae sedis* deep-bodied genera †*Analectis* and †*Natgeosocus* (Bannikov, 2014; Daniltshenko, 1980), with strata of comparable age in Germany yielding the veliferid †*Oechsleria* (Micklich & Bannikov, 2023). Unambiguous Lampridae are only known in the fossil record by the large-bodied †*Megalampris* from the Chattian (Late Oligocene) of New Zealand (Gottfried, Fordyce, & Rust, 2006) and by numerous specimens of *Lampris* from the Miocene of California (David, 1943; Jordan & Gilbert, 1919). If †*Whitephippus* is a lamprid, it would then be the first definitive Eocene representative of the family.

Ecological implications

Modern veliferid lampriforms are predominantly demersal and neritic, living at depths not exceeding 250 m (Heemstra, 1986). Their ecological habits, but also their maximum size of approximately 40 cm, differ notably from the much larger size (up to 160 cm in *Lampris* and 800 cm in *Regalecus*; Hawn and Collette 2012; Roberts 2012) and epipelagic to bathypelagic lifestyle of other lampriforms. The relatively small sized, deep bodied stem-lampriforms from the Late Cretaceous are reminiscent of veliferids and presumably had similar ecological preferences as well (Delbarre et al., 2016). In contrast, most lampriforms from the late Paleocene and early Eocene are found in formations reflecting a more open-ocean environment, such as the Thanetian-Ypresian Danata Formation of Turkmenistan and the early Ypresian Fur Formation of Denmark (Bonde et al., 2008; Schrøder, Rasmussen, Møller, & Carnevale, 2022b, 2022a), to the exception of the veliferids from the late Ypresian Bolca Lagerstätte which is reconstructed as a shallow marine reef environment (Bellwood, 1996; Marramà, Bannikov, Tyler, Zorzin, & Carnevale, 2016). Similarly, the London Clay was deposited in an open-ocean, continental shelf palaeoenvironment (King, 1981, 1984), which is

reflected by the faunal composition of its teleost fauna (Friedman et al., 2016). Based on this phylogenetic and ecological distribution, it appears likely that the putative clade formed by Lampridae and taeniosomes to the exclusion of veliferids could be characterised as a 'pelagic clade'. As a probable member of this clade, †*Whitephippus* then documents the transition in ecological preferences from proximal and demersal to oceanic and pelagic in lampriforms.

While the previous environment of the other pelagic acanthomorph clades is mostly unknown, their appearances in the fossil record are largely coordinated in time. The oldest scombrids are found in the Selandian of Angola (Dartevelle & Casier, 1949). The oldest carangids (Bannikov, 1985; Santini & Carnevale, 2015), billfishes (Fierstine, 2006; Monsch & Bannikov, 2011), and luvarids are all from the Paleocene-Eocene boundary of the Danata Formation. Deep-bodied lampriforms are also found at the latter horizon (Bannikov, 1999). The positions of these lampriform taxa are not clear, although some have suggested they might have affinities to the ‘pelagic clade’ (e.g., Near et al. 2013). Another open ocean fauna slightly older than the London Clay is found from the Fur Formation of the early Ypresian of Denmark. It preserves other *incertae sedis* lampriforms as well as scombrids, carangids and fossils attributed to other modern pelagic families such as stromateids and nomeids (Bonde, 1966; Bonde et al., 2008; Schrøder et al., 2022b). Of all the aforementioned early Palaeogene oceanic teleost faunas (to which a few other clay formations preserving fossils in three-dimensions can be added; Friedman *et al.* 2016), the London Clay is by far the most diverse: it includes gadiforms (e.g., †*Rhinocephalus*), ophidiiforms (†*Ampheristus*), trichiurids (†*Eutrichiurides*), gempylids (†*Progempylus*), scombrids (e.g., †*Eocoelopoma*, †*Micrornatus*), carangids (e.g., †*Eothynnus*), xiphioids (e.g., †*Xiphiorhynchus*) and now lampriforms with †*Whitephippus*.

Molecular studies seem to confirm the origin and rapid diversification of pelagic acanthomorph clades in the early Palaeogene (Harrington et al., 2016; Miya et al., 2013; Near et al., 2013) that is suggested by the fossil record, even if older ages of divergence are sometimes estimated (Santini & Carnevale, 2015; Santini et al., 2013; Santini & Sorenson, 2013). In particular, the taxa that occupy today the large-bodied pelagic predator ecological niche all seem to appear around the Paleocene-Eocene boundary. These taxa convergently share peculiar morphological and ecological traits that are also found in *Lampris*: relatively large body sizes, a crescentic caudal fin with the base of fin rays enveloping the caudal-fin skeleton, and a predatory behaviour that involves fast, active swimming over long distances and dives below the warm surface water. Billfishes, tunas and *Lampris* also independently developed a form of localised endothermy in the braincase, complemented in tunas and *Lampris* by a whole-body endothermy generated by axial and pectoral-fin red muscles, respectively (Dickson & Graham, 2004; Legendre & Davesne, 2020; Wegner, Snodgrass, Dewar, & Hyde, 2015). Whether †*Whitephippus* had the same kind of postcranial morphology is mostly unknown, but it might be possible to estimate if its metabolism was similar to that of modern *Lampris* by using bone histology as a proxy (Davesne, Meunier, Friedman, Benson, & Otero, 2018).

The novel attribution of †*Whitephippus* to lampriforms extends the taxon list of the early pelagic fauna of the London Clay. It reinforces the apparent observation that multiple lineages of acanthomorph teleosts simultaneously conquered the pelagic environment following the faunal depletion by the Cretaceous-Palaeogene mass extinction, separately acquiring similar morphological and physiological adaptations. Numerous taxa from the London Clay, but also from other early Palaeogene open ocean faunas (e.g., from the Fur Formation), remain poorly described and without a

precise systematic attribution. An in-depth revision of these exceptional fossils is needed to achieve a better understanding of the evolutionary dynamics underlying acanthomorph teleost diversification and the establishment of modern marine faunas.

ACKNOWLEDGEMENTS

We thank Stig Walsh (NMS), Emma Bernard and Zerina Johanson (NHMUK) for providing access to the fossil material, and Radford Arrindell (AMNH), Patrice Pruvost and Zora Gabsi (MNHN) and Randy Singer (UMMZ) for providing access to extant comparative material. Daniel Delbarre (University of Oxford) and Niels Bonde (University of Copenhagen) are thanked for their insightful discussions on the fossil specimens.

This study includes data produced in the CTEES facility at University of Michigan, supported by the Department of Earth and Environmental Sciences and the College of Literature, Science, and the Arts. This research was supported by the Natural Environment Research Council (grant NE/J022632/1 to MF), the Leverhulme Trust (grants PLP-2012-130, to MF), the University of Michigan Rackham Graduate School (Rackham Merit Fellowship to JVA), and the Alexander von Humboldt Foundation (to DD).

REFERENCES

Adolfssen, J. S., Milàn, J., & Friedman, M. (2017). Review of the Danian vertebrate fauna of southern Scandinavia. *Bulletin of the Geological Society of Denmark*, *65*, 1–23.

Agassiz, L. (1845). Report on the fossil fishes of the London Clay. *Report of the British Association, London*, *1844*, 279–310.

Alfaro, M. E., Faircloth, B. C., Harrington, R. C., Sorenson, L., Friedman, M., Thacker, C. E., … Near, T. J. (2018). Explosive diversification of marine fishes at the Cretaceous–Palaeogene boundary. *Nature Ecology & Evolution*, *2*, 688–696.

Alfaro, M. E., Santini, F., Brock, C., Alamillo, H., Dornburg, A., Rabosky, D. L., … Harmon, L. J. (2009). Nine exceptional radiations plus high turnover explain species diversity in jawed vertebrates. *Proceedings of the National Academy of Sciences*, *106*, 13410–13414.

Arambourg, C. (1943). Note préliminaire sur quelques Poissons fossiles nouveaux. *Bulletin de La Société Géologique de France*, *5*, 281–288.

Argyriou, T., & Davesne, D. (2021). Offshore marine actinopterygian assemblages from the Maastrichtian–Paleogene of the Pindos Unit in Eurytania, Greece. *PeerJ*, *9*, e10676.

Bannikov, A. F. (1985). Iskopayemye skumbrievye SSSR [Fossil scombrids of the USSR]. *Trudy Paleontologischeskogo Instituta, Akademii Nauk SSSR*, *210*, 1–111.

Bannikov, A. F. (1990). An Eocene veliferoid (Teleostei, Lampridiformes) from Bolca. *Studi e Ricerche Sui Giacimenti Terziari Di Bolca*, *6*, 161–174.

Bannikov, A. F. (1999). A review of fossil Lampridiformes (Teleostei) finds with a description of a new Lophotidae genus and species from the Oligocene of the Northern Caucasus. *Paleontological Journal*, *33*, 68–76.

Bannikov, A. F. (2014). A new genus of the family Palaeocentrotidae (Teleostei, Lampridiformes) from the Oligocene of the Northern Caucasus and comments

on other fossil Veliferoidei. *Paleontological Journal*, *48*, 624–632.
Bannikov, A. F., & Tyler, J. C. (1995). Phylogenetic revision of the fish families Luvaridae and †Kushlukiidae (Acanthuroidei), with a new genus and two new species of Eocene luvarids. *Smithsonian Contributions to Paleobiology*, *81*, 1–45.
Beckett, H. T., & Friedman, M. (2016). The one that got away from Smith Woodward: cranial anatomy of *Micrornatus* (Acanthomorpha: Scombridae) revealed using computed microtomography. *Geological Society, London, Special Publications*, *430*, 337–353.
Beckett, H. T., Giles, S., Johanson, Z., & Friedman, M. (2018). Morphology and phylogenetic relationships of fossil snake mackerels and cutlassfishes (Trichiuroidea) from the Eocene (Ypresian) London Clay Formation. *Papers in Palaeontology*, *4*, 577–603.
Bellwood, D. R. (1996). The Eocene fishes of Monte Bolca: the earliest coral reef fish assemblage. *Coral Reefs*, *15*, 11–19.
Bonde, N. (1966). The fishes of the Mo-Clay Formation (Lower Eocene). *Meddelelser Fra Dansk Geologisk Forening*, *16*, 198–202.
Bonde, N. (1995). Tidligt tertiære fisk-flere danekræ. *VARV*, 24–30.
Bonde, N., Andersen, S., Hald, N., & Jakobsen, S. L. (2008). *Danekræ - Danmarks bedste fossiler*. Copenhagen: Gyldendal.
Bonde, N., & Leal, M. E. C. (2017). Danian teleosteans of the North Atlantic Region – compared with the Maastrichtian. *Research and Knowledge*, *3*, 50–54.
Carnevale, G. (2004). The first fossil ribbonfish (Teleostei, Lampridiformes, Trachipteridae). *Geological Magazine*, *141*, 573–582.
Carnevale, G., & Bannikov, A. F. (2018). A sailfin velifer (Lampridiformes, Veliferidae) fish from the Eocene of Monte Bolca, Italy. *Bollettino Della Società Paleontologica Italiana*, *57*, 175–186.
Carnevale, G., Bannikov, A. F., Marramà, G., Tyler, J. C., & Zorzin, R. (2014). The Pesciara-Monte Postale Fossil-Lagerstätte: 2. Fishes and other vertebrates. *Rendiconti Della Società Paleontologica Italiana*, *4*, 37–63.
Casier, E. (1966). *Faune ichthyologique du London Clay*. London: British Museum (Natural History).
Cavin, L. (2001). Effects of the Cretaceous-Tertiary boundary event on bony fishes. In E. Buffetaut & C. Koeberl (Eds.), *Geological and Biological Effects of Impact Events* (pp. 141–158). Berlin: Springer.
Close, R. A., Johanson, Z., Tyler, J. C., Harrington, R. C., & Friedman, M. (2016). Mosaicism in a new Eocene pufferfish highlights rapid morphological innovation near the origin of crown tetraodontiforms. *Palaeontology*, *59*, 499–514.
Daniltshenko, P. G. (1968). Ryby verkhnego Paleotsena Turkmenyy [Fishes from the Upper Paleocene of Turkmenia]. In D. V. Obruchev (Ed.), *Ocerki po filogenii I sistematike iskopayemykh ryb I beschelyustnykh* (pp. 113–156). Moscow: Nauka.
Daniltshenko, P. G. (1980). Iskopayemyye kostistyye ryby SSSR [Fossil bony fishes of the USSR]. *Trudy Paleontologicheskogo Instituta, Akademii Nauk SSSR*, *178*.
Dartevelle, E., & Casier, E. (1949). Les poissons fossiles du Bas-Congo et des régions voisines (2e partie). *Annales Du Musée Du Congo Belge*, *2*, 257–568.
Davesne, D. (2017). A fossil unicorn crestfish (Teleostei, Lampridiformes, Lophotidae) from the Eocene of Iran. *PeerJ*, *5*, e3381.
Davesne, D., Carnevale, G., & Friedman, M. (2017). *Bajaichthys elegans* from the Eocene of Bolca (Italy) and the overlooked morphological diversity of Zeiformes

(Teleostei, Acanthomorpha). *Palaeontology*, *60*, 255–268.
Davesne, D., Friedman, M., Barriel, V., Lecointre, G., Janvier, P., Gallut, C., & Otero, O. (2014). Early fossils illuminate character evolution and interrelationships of Lampridiformes (Teleostei, Acanthomorpha). *Zoological Journal of the Linnean Society*, *172*, 475–498.
Davesne, D., Gallut, C., Barriel, V., Janvier, P., Lecointre, G., & Otero, O. (2016). The phylogenetic intrarelationships of spiny-rayed fishes (Acanthomorpha, Teleostei, Actinopterygii): fossil taxa increase the congruence of morphology with molecular data. *Frontiers in Ecology and Evolution*, *4*, 129.
Davesne, D., Meunier, F. J., Friedman, M., Benson, R. B. J., & Otero, O. (2018). Histology of the endothermic opah (*Lampris* sp.) suggests a new structure–function relationship in teleost fish bone. *Biology Letters*, *14*, 20180270.
David, L. R. (1943). Miocene fishes of Southern California. *GSA Special Papers*, *43*, 1–187.
Davis, J. W. (1890). On the fossil fish of the Cretaceous formations of Scandinavia. *Scientific Transactions of the Royal Dublin Society*, *4*, 363–434.
Delbarre, D. J., Davesne, D., & Friedman, M. (2016). Anatomy and relationships of †*Aipichthys pretiosus* and †'*Aipichthys*' *nuchalis* (Acanthomorpha: Lampridomorpha), with a review of Late Cretaceous relatives of oarfishes and their allies. *Journal of Systematic Palaeontology*, *14*, 545–567.
Dickson, K. A., & Graham, J. B. (2004). Evolution and consequences of endothermy in fishes. *Physiological and Biochemical Zoology*, *77*, 998–1018.
Fierstine, H. L. (2006). Fossil history of billfishes (Xiphioidei). *Bulletin of Marine Science*, *79*, 433–453.
Forey, P. L. (1973). A revision of the elopiform fishes, fossil and recent. *Bulletin of the British Museum (Natural History) Geology Supplement*, *10*, 1–222.
Friedman, M. (2009). Ecomorphological selectivity among marine teleost fishes during the end-Cretaceous extinction. *Proceedings of the National Academy of Sciences*, *106*, 5218–5223.
Friedman, M. (2010). Explosive morphological diversification of spiny-finned teleost fishes in the aftermath of the end-Cretaceous extinction. *Proceedings of the Royal Society B: Biological Sciences*, *277*, 1675–1683.
Friedman, M., Andrews, J. V., Saad, H., & El-Sayed, S. (2023). The Cretaceous/Paleogene transition in spiny-rayed fishes: surveying "Patterson's Gap" in the acanthomorph skeletal record. *Geologica Belgica*, *26*, 1–23.
Friedman, M., Beckett, H. T., Close, R. A., & Johanson, Z. (2016). The English Chalk and London Clay: two remarkable British bony fish *Lagerstätten*. *Geological Society, London, Special Publications*, *430*, 165–200.
Friedman, M., & Sallan, L. C. (2012). Five hundred million years of extinction and recovery: a Phanerozoic survey of large-scale diversity patterns in fishes. *Palaeontology*, *55*, 707–742.
Ghezelayagh, A., Harrington, R. C., Burress, E. D., Campbell, M. A., Buckner, J. C., Chakrabarty, P., … Near, T. J. (2022). Prolonged morphological expansion of spiny-rayed fishes following the end-Cretaceous. *Nature Ecology & Evolution*, *6*, 1211–1220.
Goodrich, E. S. (1909). Part IX. Vertebrata Craniata (First Fascicle: Cyclostomes and Fishes). In R. Lankester (Ed.), *A Treatise on Zoology*. London: Adam and Charles Black.
Gottfried, M. D., Fordyce, R. E., & Rust, S. (2006). *Megalampris keyesi*, a giant moonfish (Teleostei, Lampridiformes) from the Late Oligocene of New Zealand.

Journal of Vertebrate Paleontology, *26*, 544–551.
Grande, T., Borden, W. C., & Smith, W. L. (2013). Limits and relationships of Paracanthopterygii: A molecular framework for evaluating past morphological hypotheses. In G. Arratia, H.-P. Schultze, & M. V. H. Wilson (Eds.), *Mesozoic Fishes 5 - Global Diversity and Evolution* (pp. 385–418). Munich: Verlag Dr. Friedriech Pfeil.
Guinot, G., & Cavin, L. (2016). 'Fish' (Actinopterygii and Elasmobranchii) diversification patterns through deep time. *Biological Reviews*, *91*, 950–981.
Harrington, R. C., Faircloth, B. C., Eytan, R. I., Smith, W. L., Near, T. J., Alfaro, M. E., & Friedman, M. (2016). Phylogenomic analysis of carangimorph fishes reveals flatfish asymmetry arose in a blink of the evolutionary eye. *BMC Evolutionary Biology*, *16*, 224.
Hawn, D. R., & Collette, B. B. (2012). What are the maximum size and live body coloration of opah (Teleostei: Lampridae: *Lampris* species)? *Ichthyological Research*, *59*, 272–275.
Heemstra, P. C. (1986). Family No. 118: Veliferidae. In S. M.M. & P. C. Heemstra (Eds.), *Smith's Sea Fishes* (pp. 398–399). Berlin: Springer-Verlag.
Johnson, G. D., & Patterson, C. (1993). Percomorph phylogeny: a survey of acanthomorphs and a new proposal. *Bulletin of Marine Science*, *52*, 554–626.
Jordan, D. S., & Gilbert, J. Z. (1919). *Fossil fishes of Southern California*. Standford University, California: Stanford University Publications.
King, C. (1981). The stratigraphy of the London Clay and associated deposits. *Tertiary Research Special Papers*, *6*, 1–158.
King, C. (1984). The stratigraphy of the London clay formation and Virginia Water formation in the coastal sections of the Isle of Sheppey (Kent, England). *Tertiary Research*, *5*, 121–160.
Legendre, L. J., & Davesne, D. (2020). The evolution of mechanisms involved in vertebrate endothermy. *Philosophical Transactions of the Royal Society B: Biological Sciences*, *375*, 20190136.
Marramà, G., Bannikov, A. F., Tyler, J. C., Zorzin, R., & Carnevale, G. (2016). Controlled excavations in the Pesciara and Monte Postale sites provide new insights about the palaeoecology and taphonomy of the fish assemblages of the Eocene Bolca Konservat-Lagerstätte, Italy. *Palaeogeography, Palaeoclimatology, Palaeoecology*, *454*, 228–245.
Micklich, N., & Bannikov, A. F. (2023). *Oechsleria unterfeldensis*, gen. et sp. nov., a sailfin velifer fish (Lampridiformes, Veliferidae) from the Oligocene of the Unterfeld ("Frauenweiler") clay pit. *PalZ*, *97*, 81–104.
Miya, M., Friedman, M., Satoh, T. P., Takeshima, H., Sado, T., Iwasaki, W., … Nishida, M. (2013). Evolutionary origin of the Scombridae (tunas and mackerels): members of a Paleogene adaptive radiation with 14 other pelagic fish families. *PLoS ONE*, *8*, e73535.
Monsch, K. A. (2005). Revision of the scombroid fishes from the Cenozoic of England. *Transactions of the Royal Society of Edinburgh: Earth Sciences*, *95*, 445–489.
Monsch, K. A., & Bannikov, A. F. (2011). New taxonomic synopses and revision of the scombroid fishes (Scombroidei, Perciformes), including billfishes, from the Cenozoic of territories of the former USSR. *Earth and Environmental Science Transactions of the Royal Society of Edinburgh*, *102*, 253–300.
Müller, J. (1845). Über den Bau und die Grenzen der Ganoiden, und über das natürliche System der Fische. *Abhandlungen Der Königlichen Akademie Der*

Wissenschaften Zu Berlin, *1844*, 117–216.
Near, T. J., Dornburg, A., Eytan, R. I., Keck, B. P., Smith, W. L., Kuhn, K. L., … Wainwright, P. C. (2013). Phylogeny and tempo of diversification in the superradiation of spiny-rayed fishes. *Proceedings of the National Academy of Sciences*, *110*, 12738–12743.
Oelschläger, H. A. (1983). Vergleichende und funktionelle Anatomie der Allotriognathi (= Lampridiformes), ein Beitrag zur Evolutionsmorphologie der Knochenfische. *Abhandlungen Der Senckenbergischen Naturforschenden Gesellschaft*, *541*, 1–127.
Olney, J. E., Johnson, G. D., & Baldwin, C. C. (1993). Phylogeny of lampridiform fishes. *Bulletin of Marine Science*, *52*, 137–169.
Patterson, C. (1993). Osteichthyes: Teleostei. In M. J. Benton (Ed.), *The Fossil Record 2* (pp. 621–656). London: Chapman & Hall.
Patterson, C., & Rosen, D. E. (1977). Review of ichthyodectiform and other Mesozoic teleost fishes and the theory and practice of classifying fossils. *Bulletin of the American Museum of Natural History*, *158*, 81–172.
Roberts, T. R. (2012). *Systematics, Biology and Distribution of the Species of the Oceanic Oarfish Genus* Regalecus *(Teleostei, Lampridiformes, Regalecidae)*. Paris: Publications Scientifiques du Muséum.
Rosen, D. E. (1973). Interrelationships of higher euteleostean fishes. In P. H. Greenwood, R. S. Miles, & C. Patterson (Eds.), *Interrelationships of Fishes* (pp. 397–513). London: Academic Press.
Sabaj, M. H. (2020). Codes for natural history collections in ichthyology and herpetology. *Copeia*, *108*, 593–669.
Santini, F., & Carnevale, G. (2015). First multilocus and densely sampled timetree of trevallies, pompanos and allies (Carangoidei, Percomorpha) suggests a Cretaceous origin and Eocene radiation of a major clade of piscivores. *Molecular Phylogenetics and Evolution*, *83*, 33–39.
Santini, F., Carnevale, G., & Sorenson, L. (2013). First molecular scombrid timetree (Percomorpha: Scombridae) shows recent radiation of tunas following invasion of pelagic habitat. *Italian Journal of Zoology*, *80*, 210–221.
Santini, F., & Sorenson, L. (2013). First molecular timetree of billfishes (Istiophoriformes: Acanthomorpha) shows a Late Miocene radiation of marlins and allies. *Italian Journal of Zoology*, *80*, 481–489.
Schrøder, A. E., Rasmussen, J. A., Møller, P. R., & Carnevale, G. (2022a). A new beardfish (Teleostei, Polymixiiformes) from the Eocene Fur Formation, Denmark. *Journal of Vertebrate Paleontology*, *42*, e2142914.
Schrøder, A. E., Rasmussen, J. A., Møller, P. R., & Carnevale, G. (2022b). *Butyrumichthys henricii* gen. et sp. nov.: a new stromateiform fish from the lower Eocene Fur Formation, Denmark. *Journal of Vertebrate Paleontology*, *42*, e2171798.
Sorbini, L., & Bottura, C. (1988). *Bajaichthys elegans*, an Eocene lampridiform from Bolca (Italy). *Bollettino Del Museo Civico Di Storia Naturale Di Verona*, *14*, 369–380.
Underkoffler, K. E., Luers, M. A., Hyde, J. R., & Craig, M. T. (2018). A taxonomic review of *Lampris guttatus* (Brünnich 1788) (Lampridiformes; Lampridae) with descriptions of three new species. *Zootaxa*, *4413*, 551–565.
Walters, V. (1957). *Protolophotus*, a new genus of allotriognath fish from the Oligocene of Iran. *Copeia*, *1*, 60–61.
Wang, J., Yu, H., Ma, S., Lin, Q., Wang, D., & Wang, X. (2023). Phylogenetic and

evolutionary comparison of mitogenomes reveal adaptive radiation of lampriform fishes. *International Journal of Molecular Sciences*, *24*, 8756.

Wegner, N. C., Snodgrass, O. E., Dewar, H., & Hyde, J. R. (2015). Whole-body endothermy in a mesopelagic fish, the opah, *Lampris guttatus*. *Science*, *348*, 786–790.

Wiley, E. O., Johnson, G. D., & Dimmick, W. W. (1998). The phylogenetic relationships of lampridiform fishes (Teleostei: Acanthomorpha), based on a total-evidence analysis of morphological and molecular data. *Molecular Phylogenetics and Evolution*, *10*, 417–425.

Woodward, A. S. (1901). *Catalogue of Fossil Fishes in the British Museum (Natural History). Part IV. Containing the Actinopterygian Teleostomi of the Suborders Isospondyli (in Part), Ostariophysi, Apodes, Percesoces, Hemibranchii, Acanthopterygii, and Anacanthini*. London: British Museum (Natural History).